

DESIGN , ANALYSIS AND MATHEMATICAL MODELLING OF WIDEBAND PHASE SHIFTER

Dissertation submitted in fulfillment of the requirements for the Degree

MASTERS OF TECHNOLOGY IN ELECTRONICS & COMMUNICATION ENGINEERING

by

Vishakha Thakur

162003

Under the Supervision of

Dr. Salman Raju Talluri

and

Dr. Meenakshi Sood



DEPARTMENT OF ELECTRONICS AND COMMUNICATION ENGINEERING
JAYPEE UNIVERSITY OF INFORMATION TECHNOLOGY WAKNAGHAT, SOLAN -
173234, INDIA

May – 2018

Contents

Declaration	iii
Supervisor Certificate	iv
Acknowledgment	v
Abstract	vi
List of Figures	vii
List of Tables	x
List of Abbreviations	xi
List of Symbols	xii
Chapter 1. INTRODUCTION	1
1.1. Literature Review	1
1.2. Objectives	4
Chapter 2. ANALYSIS OF BRANCH LINE COUPLER	5
2.1. Mathematical analysis of branch line coupler	5
Chapter 3. MINIATURIZATION OF BRANCH LINE COUPLER	10
3.1. Stubs in the horizontal branches	10
3.2. Stubs in the vertical branches	20
3.3. Stubs in vertical and horizontal branches	30
3.4. Miniaturized branch line coupler	35
Chapter 4. REALIZATION OF WIDE BAND BRANCH LINE COUPLER USING FILTERS COEFFICIENTS	41
4.1. Branch line coupler with third order filters	42
4.2. Branch line coupler with fifth order filters	43
Chapter 5. IMPEDANCE VARIATION OF BRANCH LINE COUPLER	46
5.1. Variation in impedance of middle line of branch line coupler	47
Chapter 6. CONCLUSION	54
Bibliography	55

Declaration

Declaration By The Scholar

I hereby declare that the work reported in the M.Tech dissertation entitled “**DESIGN , ANALYSIS AND MATHEMATICAL MODELLING OF WIDEBAND PHASE SHIFTER**” submitted at **Jaypee University of Information Technology, Wagnaghat India**, is an authentic record of my work carried out under the guidance of **Dr. Salman Raju Talluri** and **Dr Meenakshi Sood**. I have not submitted this work elsewhere for any other degree or diploma.

Vishakha Thakur

Vishakha Thakur

Department of Electronics and Communication Engineering

Jaypee University of Information Technology, Wagnaghat, India

Date: *10-May-2018*

Supervisor Certificate

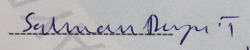


JAYPEE UNIVERSITY OF INFORMATION TECHNOLOGY

(Established by H.P. State Legislative vide Act No. 14 of 2002)
P.O. Wahnaghat, Teh. Kandaghat, Distt. Solan - 173234 (H.P.) INDIA
Website: www.juit.ac.in
Phone No. (91) 01 792-257999
Fax: +91-01792-245362

Supervisor's Certificate

This is to certify that the work reported in the M.Tech project report entitled **"DESIGN, ANALYSIS AND MATHEMATICAL MODELLING OF WIDEBAND PHASE SHIFTER"** which is being submitted by **Vishakha Thakur** in fulfillment for the award of Masters of Technology in Electronics and Communication Engineering by the Jaypee University of Information Technology, is the record of candidate's own work carried out by her under our supervision. This work is original and has not been submitted partially or fully anywhere else for any other degree or diploma.



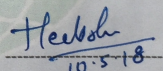
Dr. Salman Raju Talluri

Assistant Professor

ECE Department

JUIT

Date 10 May, 2018



Dr. Meenakshi Sood

Assistant Professor

ECE Department

JUIT

Date 10-May-2018

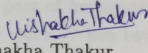
Acknowledgment

Acknowledgment

I would like to express deep gratitude to my guide **Dr. Salman Raju Talluri** and co-guide **Dr. Mennakshi Sood** for their unlimited support, useful critiques and guidance. Their valuable advice and suggestions encouraged me in numerous ways. My special thanks to **Prof. (Dr.) Samir Dev Gupta** Director and Head of ECE Department, for providing all the facilities.

I would like to extend my thanks to all the faculty members of the department and lab staff, for their constant encouragement during the project. I also take the opportunity to thank all my friends who were always been there for me whenever I needed their support and help. They have directly or indirectly helped me in my work. Finally I would like to take the opportunity to thank my parents for their moral support and continuous encouragement.

Date: 10-May-2018


Vishakha Thakur

Abstract

Phase shifters have wide demand in microwave communication system, such as phased array antenna and beam forming networks. For all the mentioned applications, miniaturized structure, control over the gains of the phase shifters and wide band response of the phase shifters are the need of the modern era. This research work presents the design and analysis of branch line coupler that is operating at 3 GHz frequency and is providing 90° phase shift between the two ports. To miniaturize the structure, stubs are introduced in the unutilized space of branch line coupler. To make its response wide band, horizontal branches of the branch line coupler are replaced with different filter coefficients. Another application of branch line coupler is explored by varying the impedance of its horizontal branch.

In the miniaturized branch line coupler design, by adding the stubs 39% of size reduction is achieved as compared to the conventional branch line coupler. Upon replacing the branch line coupler with Butterworth filter coefficients, the fractional achieved is more than 80%. After this gain of branch line coupler is varied by impedance variation of only a part of horizontal line and optimum value of 100 ohms is chosen, as the maximum impedance value. When two modified structure are used such that one is mirror image of the other, for feeding the antenna, it can be used for target detection in radar systems.

List of Figures

2.0.1	Geometry of branch line coupler	5
2.1.1	Circuit of normalized branch line coupler	6
2.1.2	Branch line coupler	8
2.1.3	Simulation results of magnitude and phase response of branch line coupler	9
3.1.1	Circuit of single shunt stub branch line coupler	11
3.1.2	Simulation results of variable impedance for single stub	13
3.1.3	Simulation results of single stub with variable length	14
3.1.4	Circuit of double shunt stubs branch line coupler	14
3.1.5	Simulation results of variable impedance for double stub	15
3.1.6	Simulation results of variable length for two stubs branch line coupler	16
3.1.7	Circuit of three shunt stubs branch line coupler	17
3.1.8	Simulation results of variable impedance for three stubs	17
3.1.9	Simulation results of variable length for three stubs branch line coupler	18
3.1.10	Circuit of five shunt stubs branch line coupler	18
3.1.11	Simulation results of variable impedance for five stubs	19
3.1.12	Simulation results of variable length for five stubs branch line coupler	20
3.2.1	Circuit of two vertical stubs branch line coupler	20
3.2.2	Simulation results of variable impedance for two vertical stubs	23
3.2.3	Simulation results of variable length for two vertical stubs branch line coupler	24
3.2.4	Circuit of branch line coupler with four vertical stubs	25
3.2.5	Simulation results of variable impedance for four vertical stubs	28
3.2.6	Simulation results of variable length for four vertical stubs branch line coupler	29
3.2.7	Circuit of branch line coupler with five vertical stubs	29
3.3.1	Circuit of branch line coupler with four stubs in vertical branch and one stub in horizontal branch	31

3.3.2	Simulation results of branch line coupler with four stubs in vertical branch and one in horizontal branch	31
3.3.3	Simulation results of variable length for four vertical stubs and one horizontal stub branch line coupler	32
3.3.4	Circuit diagram of miniaturized branch line coupler with five stubs in horizontal branches and four stubs in vertical branches	33
3.3.5	Simulation results of branch line coupler with four stubs in vertical branch and five in horizontal branch	33
3.3.6	Simulation results of variable length for four vertical stubs and five horizontal stub branch line coupler	34
3.4.1	Matlab simulation result of comparison of miniaturized branch line coupler with conventional branch line coupler	35
3.4.2	CST structure of miniaturized branch line coupler	36
3.4.3	CST simulation results of miniaturized branch line coupler	37
3.4.4	Mapping of CST and Matlab simulation results	37
3.4.5	Circuit diagram of branch line coupler with five stubs on each branch	38
3.4.6	Matlab simulation result of branch line coupler with five stubs on each branch	38
3.4.7	CST structure of miniaturized branch line coupler five vertical stubs on each branch	39
3.4.8	CST simulation result of miniaturized branch line coupler with five stubs on each branch	39
3.4.9	Mapping of CST and Matlab simulation results of miniaturized BLC	40
4.1.1	Matlab simulation results of BLC with third order filter	42
4.1.2	Phase response of BLC with third order Butterworth and Equiripple filters	43
4.2.1	Matlab simulation results of BLC with fifth order filters	43
4.2.2	Phase response of BLC replaced with Butterworth, Equiripple and Binomial fifth order filters	44
5.0.1	Circuit of branch line coupler for impedance variation	46
5.0.2	Variation of S-parameters of BLC with varying impedance of complete horizontal line	46
5.1.1	Variation of S-parameters of BLC with impedance variation	47
5.1.2	Circuit diagram of modified branch line coupler	48
5.1.3	CST layout of modified BLC	49
5.1.4	Simulation results of conventional and modified branch line coupler	49

5.1.5	Phase responses of conventional and modified branch line coupler	50
5.1.6	Excitation for difference and sum patterns using modified BLC in antenna arrays	50
5.1.7	Sum and difference pattern of simple antenna array, conventional branch line coupler and modified branch line coupler	51
5.1.8	Difference between sum and difference patterns	52

List of Tables

1	Comparison of S-parameters for different values of impedance	14
2	Comparison of S-parameters for different values of impedance for two stubs	16
3	Comparison of S-parameters for different values of impedance for three stubs	18
4	Comparison of S-parameters for different values of impedance for five stubs	19
5	Comparison of S-parameters for different values of impedance for two vertical stubs	24
6	Comparison of S-parameters for different values of impedance for four vertical stubs	28
7	Comparison of S-parameters of branch line coupler with four stubs in vertical branch and one in horizontal branch	32
8	Comparison of S-parameters of branch line coupler with four stubs in vertical branch and five in horizontal branch	34
9	Properties of RT-Duroid 5880	36
10	Design parameters of miniaturized branch line coupler	36
1	Comparison of BLC with 3rd order filters	42
2	Comparison of BLC with 5th order filters	44
1	Design parameters of modified branch line coupler	48
2	Phase and gain of sum and difference patterns of simple BLC	51
3	Phase and gain of sum and difference patterns of modified BLC	52
4	Regions for target detection with modified branch line coupler in antenna array	52
5	Regions for target detection in simple antenna array	53

List of Abbreviations

BLC= Branch Line Coupler

CST = Computer Simulation Technology

dB= Decibel

GHz= Giga Hertz

MHz= Mega Hertz

mm= Millimeter

List of Symbols

c = Speed of light

f = Frequency

β = Phase constant

λ = Wavelength

μ_r = Relative permeability

ξ = Relative permittivity

ξ_{eff} = Effective relative permittivity

Γ_e = Reflection coefficient of even mode

Γ_o = Reflection coefficient of odd mode

Ω = Ohms

CHAPTER 1

INTRODUCTION

A phaseshifter is a device that changes the phase of a signal. When a wave is made to pass through it, it provides a phase variation in the wave at its output ports [1]. Phaseshifters can be designed to provide any phase shift between the output ports by changing the dimensions of phaseshifter. In many microwave applications phase shifter is a critical component. It find its applications mainly in phased array antenna and beam forming networks. Phased array antenna can control the direction of wave beam without the need to change the position of antenna elements. Phased array antenna consists of many antenna elements. Each antenna element contain phaseshifter in them which control the phase of the signal that is entering the antenna system. Light weight, small size and low cost phaseshifters are important for designing the phased array antenna [2].

Another application of phaseshifter is that they are used in power division and coupling. In power division the power of the input signal can be divided into two output signals. Power division can be a equal power division or unequal power division. In power coupling power of two input signals are combined [3].

1.1. Literature Review

In [4], authors have replaced the branches of branch line coupler with dual transmission lines and partial meandering lines. The miniaturized coupler is operating at 1.675 GHz frequency. The presented design able to give the equal power division between two output ports

Authors in [5] have replaced all the branches of conventional coupler with transmission line with three open circuited stubs from which one is center tapped and two are end-tapped open circuited stubs. Thereby achieving the reduced size with harmonic suppression. A branch line coupler was also designed operating at 1 GHz , which occupies 56% of circuit area of the conventional coupler

In [6] new miniaturized branch line coupler is presented at 0.7 GHz frequency by using composite right/left handed transmission line structures which has meander shaped slots. The structure contained in 22.8% area of traditional coupler.

In [7] authors have used dual transmission in place of quarter wavelength line of conventional coupler, where one transmission line that is of quarter wavelength is smaller than other at 2.4 GHz frequency. The miniaturized coupler is narrower than the traditional branch line coupler. 63.9% of size reduction rate have been achieved compared to convention branch line coupler.

Authors in [8] have modified the structure of conventional branch line coupler by adding small transmission line sections at all the ports and thereby extending to the ports to achieve dual band functionality of the coupler. Coupler still providing 90° at the two bands of frequencies i.e 1 GHz and 2 GHz .

In [9], in place of simple transmission line the proposed coupler is using artificial transmission lines i.e stubs are added between each quarter wavelength line of branch line coupler. Proposed branch line coupler has 49%-63% of size compared to conventional branch line coupler and miniaturized rat-race has 32%-46% of size compared to conventional rat-race coupler.

Authors in [10], have miniaturized the structure of branch line coupler by adopting a fractal geometry, thereby reducing the space of microstrip line. Along with fractal geometry miniaturized stubs are also used to achieve miniaturized structure. The proposed coupler is operating at 880 MHz frequency

In [11] paper, a quad band rat-race coupler was designed for suppressing the spurious passbands. For this purpose laterally offset dual ring resonators were used with concentric dual split rings. At frequencies 1.45 GHz , 3.8 GHz , 4.3 GHz and 6.3 GHz quadband response was obtained from designed structure.

In [12] open circuited stubs are used in the structure that are added in the structure, that are added on every branch of the coupler. These center tapped stubs are used to reduce the structure size and suppress the harmonics. Structure still providing the characteristic of conventional branch line coupler.

In [13] wide banding of branch line coupler is done only by doing simple modification and that is adding open coupled line of quarter wavelength, near every feed line. There by 49% of fractional bandwidth is achieved.

In [14] very simple modification in the conventional structure of branch line coupler is done and that is adding a transmission line section of quarter wavelength at each port, to achieve wideband properties. Along with this another method also has been explored in which the intentional mismatch was introduced to improve the bandwidth even more. 50.9% of bandwidth have been achieved.

In [15] authors have designed dual band branch line coupler by integrating T network. This dual band branch line coupler is designed with unequal branch lengths. To demonstrate the viability of the structure, a wide frequency ratio crossover is designed with simple layout. Proposed method was used to design branch line coupler with unequal power division.

In [16], parallel coupled three line are used in the center of two section branch line coupler to make the coupler wideband. The fractional bandwidth of the proposed structure provides the wider bandwidth compared to two section branch line coupler and also wider bandwidth than three section branch line coupler with 55% of fractional bandwidth.

In [17], stubs were introduced in a high impedance line and low impedance line to control the characteristic impedance of two section branch line coupler such that higher impedance should remain below 100Ω , which can be easily fabricated using ordinary planar technology.

In [18] authors have utilized the branch line bidirectional coupler to design microwave band pass filter. Thereby exploring another application of branch line coupler. For utilizing the branch line coupler as a band pass filter, it is utilized as transversal filtering section, by introducing the open circuited transmission line section at the coupled port of branch line coupler and taking output from the isolated port. By changing the design parameter of the transversal section bandwidth along with position of out of band can be controlled. Bandpass filter operating at 5 GHz frequency was designed.

In [19], dual band branch line coupler is designed using simplified composite right/left handed transmission lines for arbitrary power division. These simplified composite right/left handed transmission line can be easily modified to match the conventional 90° sections at two frequencies that are 2.45 GHz to 5.2 GHz .

In [20], eight open ended resonator are embedded inside the hybrid coupler. The new design uses ring resonator which suppress the sixth harmonic with miniaturization of 20.4% at 0.96 GHz .

In [21] authors have designed dual band 90° hybrid with arbitrary coupling. The method that is used to achieve this arbitrary coupling is, introducing four or two stubs at different locations of branch line coupler. Three designs of branch line coupler have been fabricated. In first design stubs are adding at the starting of quarter wavelength lines, in second and third structure stubs are adding in the middle of the vertical branches of the coupler operating at 2.45/3/9 GHz .

Authors in [22] have investigated two branch lumped element based branch line coupler for impedance transformation. Branch line coupler of $\frac{\lambda}{4}$ or $\frac{3\lambda}{4}$ wavelength based on lumped element coupler which has only six elements are discussed. The value of these lumped elements are determined by two factor that are coupling factor and other is terminal load admittance.

Authors in [23] have designed a dual band 90° hybrid coupler for equal power division at the two frequencies. In the design, transmission line of conventional hybrids are transformed to pi-equivalent circuit. By this method power division of 1:1 and 1:3 are obtained.

In [24], a branch line coupler operating at 430 MHz has been designed with unequal amplitudes. This is achieved by varying the impedance of the one of the arms of 90° coupler. This coupler finds its application in shared aperture antenna, beam forming network and feeder network and other radar application operating at 430 MHz .

In [25], a three way power divider with unequal power distribution is designed using wilkinson power divider. This is done by integrating the dual band power integrating the dual band power divider cell along with the two section transformer for dual frequency. The two frequencies at which designed divider operates are 0.6 and 2.45 GHz .

In [26] authors have designed a simple ring shaped coupler with the transmission line section of impedance 50 Ω for unequal power division. Unequal power division is changed by varying the electrical length of 50 Ω line without the need to vary the impedance.

In [27] authors develops a design procedure for different input and output impedance matching of a asymmetrical multi section power divider. For this purpose firstly the circuit

was designed and S-parameters of the circuit were determined, then by the means of least mean square method error function was calculated.

In [28] authors have incorporated isolation impedance at different locations with in quarter wavelength transmission lines. This is serving two purposes one is that it is producing physical separation between two output ports and other purpose is that it is providing electrical isolation between two output ports.

In [29], dual band branch line is designed with port extension by using Riblet's concept. To achieve wider band ratio the structure was incorporated improved matching of the ports impedance.

In [30], branch line coupler was designed for arbitrary coupling. To achieve this arbitrary coupling variation in only the electrical length of the branch line coupler has been done. Impedance of the branch line coupler remain exactly same. By this method wide range of values can be achieved.

After reviewing all these literature it is concluded that miniaturization of branch line coupler by replacing the shunt arms with partially meandering lines and dual transmission line is done in [4] but it adds discontinuities to the structure. Another method is to add complementary split ring resonator in between the branches of conventional coupler [6]. This coupler is only be useful for narrow band applications. Structure proposed in [10] for miniaturization is complex. In [19] authors presents a complex design to achieve unequal power division. Keeping the above modifications in mind following objectives are formed.

1.2. Objectives

The major motivation behind this project is the need of phase shifter in various applications such as in antenna arrays and beam forming network. For phase shifter to perform its best in various applications, requires rigorous analysis of various phase shifters. Thus to facilitate the need of phase shifter to perform according to modern applications, following objectives were formed.

- Design and analysis of Branch line coupler
- Miniaturization of branch line coupler by introducing shunt stub (Design parameter are Number of stubs, length of stubs and impedance of stub)
- To develop a new approach for realization of wide band branch line coupler
- To achieve unequal power division using the same phaseshifter

Rest of the thesis is organized in the following manner. In Chapter two mathematical analysis and design of branch line coupler is done. In Chapter three miniaturization of branch line coupler is done by introducing stubs. In Chapter four a method is proposed to make the branch line coupler response wideband. In Chapter five another application of branch line coupler is explored by small impedance variation in the coupler's structure.

CHAPTER 2

ANALYSIS OF BRANCH LINE COUPLER

In many microwave applications, phaseshifters plays an important role. Phase shifter can be used for power division and power coupling [3]. Two basic type of phase shifters are 90° and 180° hybrid. The 90° hybrid also known as branch line coupler (BLC), is basically a four port network, two input ports and two output ports. As the name suggest, the 90° hybrid provides 90° phase shift between two output ports. When the power is entering to the port one, as shown in figure 2.0.1, then the output is equally divided in port two and port three, with phase difference of 90° between them. Port four is isolated. Branch line coupler has dimension in quarter wavelength ($\frac{\lambda}{4}$)[3]

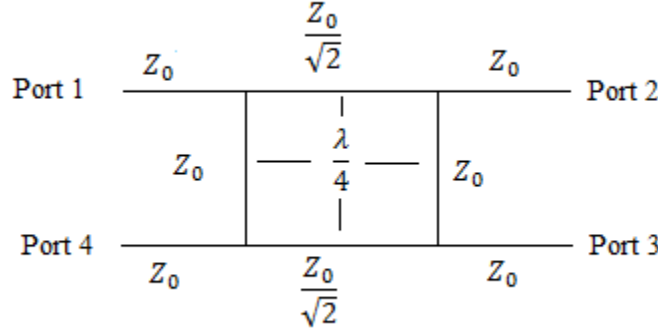


FIGURE 2.0.1. Geometry of branch line coupler

2.1. Mathematical analysis of branch line coupler

For analyzing the response of any phase shifter or any other microwave device, S-parameters plays an important role. It also provides information about the transmission and reflection coefficients. In other words S-parameters provides a relation between the voltage incident on the port to the voltage reflected from the port [31]

$$(2.1.1) \quad S_{ij} = \frac{V_i^-}{V_j^+}$$

When $V_k^+ = 0$ for $k \neq j$ this signifies that j^{th} port is not matched but rest of the ports are matched

where j is the input port and i is the output port, S_{ij} is element of scattering matrix. S_{ij} can be found by driving port j with an incident wave of voltage V_j^+ and measuring the amplitude of the reflected wave V_i^- . S_{ii} is the reflection coefficient and S_{ij} is the transmission coefficient[3].

S matrix of branch line coupler is given as

$$(2.1.2) \quad [S] = -\frac{1}{\sqrt{2}} \begin{bmatrix} 0 & j & 1 & 0 \\ j & 0 & 0 & 1 \\ 1 & 0 & 0 & j \\ 0 & 1 & j & 0 \end{bmatrix}$$

For mathematical analysis of branch line coupler even odd mode analysis needs to be done. Firstly all the transmission lines are normalized with characteristic impedance Z_0 then the circuit is divided horizontally into set of two, two port networks. The wave is incident on port 1, after the circuit is decomposed into even and odd mode excitation. The total excitation of the complete circuit can be calculated by superimposing the two excitation [3].

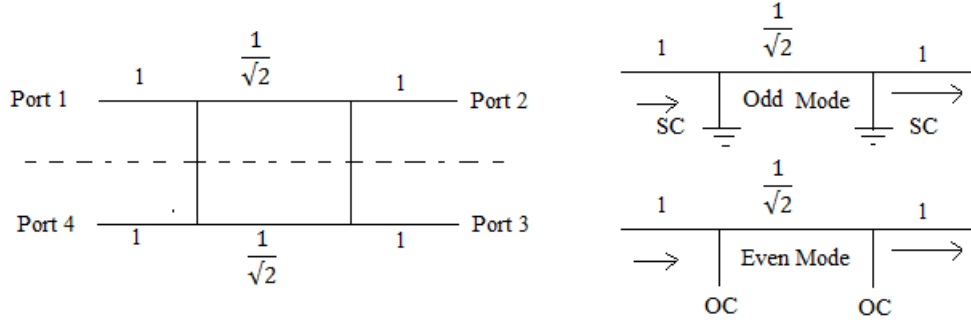


FIGURE 2.1.1. Circuit of normalized branch line coupler

$$(2.1.3) \quad S_{11} = \frac{(\Gamma_e + \Gamma_o)}{2}$$

$$(2.1.4) \quad S_{12} = \frac{(T_e + T_o)}{2}$$

$$(2.1.5) \quad S_{13} = \frac{(T_e - T_o)}{2}$$

$$(2.1.6) \quad S_{14} = \frac{(\Gamma_e - \Gamma_o)}{2}$$

where the Γ_e and Γ_o are even and odd mode reflection coefficients and T_e and T_o is even and odd mode transmission coefficients.

2.1.1. Even mode analysis. For calculating the the even mode reflection and transmission coefficient multiplication of ABCD matrix of all the cascaded elements is done.

Length of the shunt stub (l)

$$(2.1.7) \quad l = \frac{\lambda}{8}$$

Phase constant (β)

$$(2.1.8) \quad \beta = \frac{2\pi}{\lambda}$$

$$(2.1.9) \quad Y = -jZ_0 \cot(\beta l) = -j$$

ABCD matrix of shunt stub

$$\begin{bmatrix} A & B \\ C & D \end{bmatrix}_{stub} = \begin{bmatrix} 1 & 0 \\ j & 1 \end{bmatrix}$$

and ABCD matrix of transmission line

$$\begin{bmatrix} A & B \\ C & D \end{bmatrix}_{txline-even} = \begin{bmatrix} 0 & \frac{j}{\sqrt{2}} \\ j\sqrt{2} & 0 \end{bmatrix}$$

ABCD matrix of even mode cascaded elements

$$\begin{bmatrix} A & B \\ C & D \end{bmatrix} = \begin{bmatrix} 1 & 0 \\ j & 1 \end{bmatrix} \begin{bmatrix} 0 & \frac{j}{\sqrt{2}} \\ j\sqrt{2} & 0 \end{bmatrix} \begin{bmatrix} 1 & 0 \\ j & 1 \end{bmatrix} = \begin{bmatrix} \frac{-1}{\sqrt{2}} & \frac{j}{\sqrt{2}} \\ \frac{j}{\sqrt{2}} & \frac{-1}{\sqrt{2}} \end{bmatrix}$$

$$(2.1.10) \quad \Gamma_e = \frac{A + B - C - D}{A + B + C + D} = 0$$

$$(2.1.11) \quad T_e = \frac{2}{A + B + C + D} = \frac{-1}{\sqrt{2}} (1 + j)$$

2.1.2. Odd mode analysis. Similar steps are followed for calculating reflection and transmission coefficient for odd case.

$$(2.1.12) \quad Y = jZ_0 \tan(\beta l) = j$$

$$\begin{bmatrix} A & B \\ C & D \end{bmatrix}_{txline-odd} = \begin{bmatrix} \frac{1}{\sqrt{2}} & \frac{j}{\sqrt{2}} \\ \frac{j}{\sqrt{2}} & \frac{1}{\sqrt{2}} \end{bmatrix}$$

$$(2.1.13) \quad \Gamma_e = \frac{A + B - C - D}{A + B + C + D} = 0$$

$$(2.1.14) \quad T_e = \frac{2}{A + B + C + D} = \frac{1}{\sqrt{2}} (1 - j)$$

By using above equations

$$(2.1.15) \quad S_{11} = 0$$

$$(2.1.16) \quad S_{12} = \frac{-j}{\sqrt{2}}$$

$$(2.1.17) \quad S_{13} = \frac{-1}{\sqrt{2}}$$

$$(2.1.18) \quad S_{14} = 0$$

From 2.1.16 and 2.1.17 it can be observed that half power is delivered to port 2 and angle is 90 degree, rest half is delivered to port 3 and angle between port three and port one is 180 degrees [3].

2.1.3. Design of branch line coupler. The branch line coupler is designed for 3 GHz whose wavelength can be calculated as

$$(2.1.19) \quad \lambda = \frac{c}{f \sqrt{\mu_r \epsilon_{eff}}}$$

where c is speed of light ($c = 3 \times 10^8$) m/s, f is the operating frequency ($f = 3$ GHz), μ_r is relative permeability ($\mu_r = 1$) and ϵ_{eff} is effective relative permittivity ($\epsilon_{eff} = \sqrt{1.7}$).

The structure is designed in Full wave EM simulator (CST microwave studio) [32].

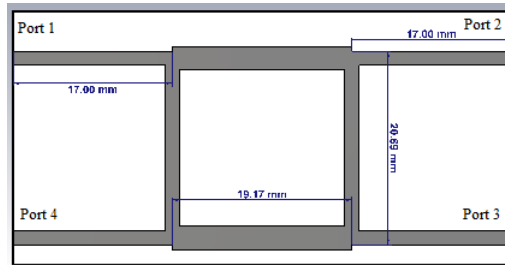


FIGURE 2.1.2. Branch line coupler

The structure is placed on the material RT-Duroid 5880, with dielectric constant 2.2 and the substrate height (0.508mm). Here the impedance of feeding line is 50Ω , line impedance is 35.35Ω , length of feeding line and line length is mentioned in figure 2.1.2, width of feeding line and line length is (1.5mm) and (2.5mm) respectively and conductor thickness is taken as (0.035mm).

Figure 2.1.3 shows the magnitude and phase responses of branch line coupler.

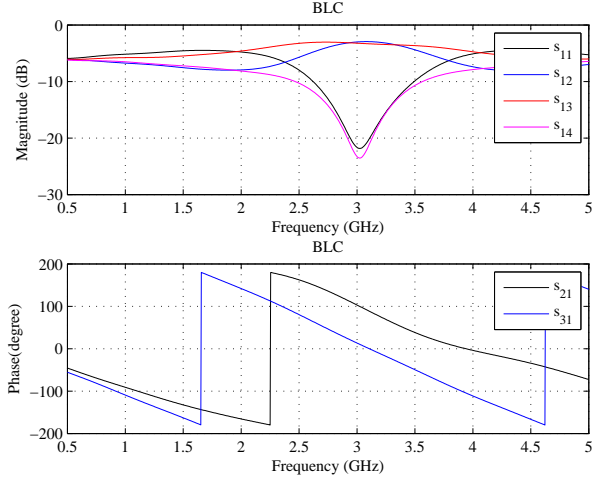


FIGURE 2.1.3. Simulation results of magnitude and phase response of branch line coupler

Magnitude of S_{12} is -3.16 dB , S_{13} is -3.06 dB , S_{11} is -22.79 dB and S_{14} is -23.186 dB . The angle of S_{21} is 93.5° , S_{31} is 3.14° so difference between angle of S_{12} and S_{13} is 90.3° . As the magnitude of S_{12} and S_{13} is approximately 3 dB therefore it is clear that this coupler is providing equal power division at its output ports (i.e port 2 and port 3).

This coupler is designed to operate at 3 GHz and the structure dimensions are 19.17 mm . For certain applications the working frequency is less than 3 GHz and coupler is frequently used in those applications. At lower frequencies the dimensions of the branch line coupler increases because of the inverse relationship between the frequency and wavelength. So the miniaturized design is presented in the next chapter.

CHAPTER 3

MINIATURIZATION OF BRANCH LINE COUPLER

This phase shifter (Branch line coupler) uses significant amount of circuit area, it has dimension of quarter wavelength ($\frac{\lambda}{4}$). At low frequencies the λ increases so dimension of branch line coupler also increases.

$$(3.0.1) \quad \lambda = \frac{c}{f}$$

where c is speed of light ($c = 3 \times 10^8$)m/s, f is the frequency

Therefore in this case miniaturization of this phase shifter needs to be done [9].

In this report work miniaturization of branch line coupler is done by adding shunt stubs in the vertical and horizontal branches. Adding stubs is leading to miniaturization because shunt stubs are increasing the capacitance of circuit which is leading to decrease in resonance frequency. The characteristic impedance Z_0 of transmission line and phase velocity v_p are defined as

$$(3.0.2) \quad Z_0 = \sqrt{\frac{L}{C}}$$

$$(3.0.3) \quad v_p = \frac{1}{\sqrt{LC}}$$

where L and C are the inductance and capacitance per unit length of the line. Phase velocity can also be expressed in terms of propagation constant β and angular frequency ω as

$$(3.0.4) \quad v_p = \frac{\omega}{\beta}$$

So it is clear from above equations that if capacitance increases, phase velocity decreases, wavelength decreases and that's how the miniaturization is achieved.

3.1. Stubs in the horizontal branches

For miniaturization of branch line coupler the stubs are added in the horizontal branches of branch line coupler.

3.1.1. Single shunt stub. Firstly only one shunt stub is connected in the middle, because of which, horizontal line of branch line coupler gets divided into two equal parts. Circuit of branch line coupler with single shunt stub is shown in figure 3.1.1.

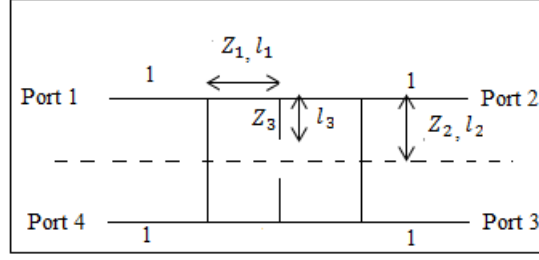


FIGURE 3.1.1. Circuit of single shunt stub branch line coupler

Length of the original shunt stub (l_2) and impedance of original stub (Z_2) are $l_2 = \frac{\lambda}{8}$ and $Z_2 = 1$ respectively. Length of transmission line (l_1) and impedance of transmission line are $l_1 = \frac{\lambda}{8}$ and $Z_1 = \frac{1}{\sqrt{2}}$ respectively.

Phase constant (β)

$$(3.1.1) \quad \beta = \frac{2\pi}{\lambda}$$

3.1.1.1. *Even mode analysis.* For calculating the the even mode reflection and transmission coefficients, multiplication of ABCD matrix of all the cascaded elements is done.

$$(3.1.2) \quad Z_{in1} = -jZ_2 \cot(\beta l_2)$$

$$(3.1.3) \quad Z_{in2} = -jZ_3 \cot(\beta l_3)$$

ABCD matrix of original shunt stub of length l_2 is

$$(3.1.4) \quad [A_1] = \begin{bmatrix} 1 & 0 \\ \frac{1}{Z_{int1}} & 1 \end{bmatrix}$$

ABCD matrix of transmission line

$$(3.1.5) \quad [A_2] = \begin{bmatrix} \cos(\beta l_1) & jZ_1 \sin(\beta l_1) \\ j\frac{1}{Z_1} \sin(\beta l_1) & \cos(\beta l_1) \end{bmatrix}$$

ABCD matrix of added shunt stub of length l_3 is given by

$$(3.1.6) \quad [A_4] = \begin{bmatrix} 1 & 0 \\ \frac{1}{Z_{int2}} & 1 \end{bmatrix}$$

ABCD matrix of even mode cascaded elements

$$(3.1.7) \quad [A_3] = \begin{bmatrix} A & B \\ C & D \end{bmatrix} = [A_1] [A_2] [A_4] [A_2] [A_1]$$

Reflection coefficient of even mode can be calculated as

$$(3.1.8) \quad \Gamma_e = \frac{A + B - C - D}{A + B + C + D}$$

Transmission coefficient of even mode can be calculated as

$$(3.1.9) \quad T_e = \frac{2}{A + B + C + D}$$

The analysis of this circuit is done by varying two parameters, one is impedance of the shunt stub and other is length of the shunt stub.

3.1.1.2. *Odd mode analysis.* Similar steps needs to be followed for calculating reflection and transmission coefficients for odd case.

$$(3.1.10) \quad Z_{in3} = jZ_2 \tan(\beta l_2)$$

and impedance of added shunt stub of length l_3 is given in 3.1.3

ABCD matrix of original shunt stub of length l_2

$$(3.1.11) \quad [A_{11}] = \begin{bmatrix} 1 & 0 \\ \frac{1}{Z_{int3}} & 1 \end{bmatrix}$$

ABCD matrix of transmission line and added stub are given in 3.1.5 and 3.1.6 respectively. ABCD matrix of odd mode cascaded elements

$$(3.1.12) \quad [A_3] = \begin{bmatrix} A & B \\ C & D \end{bmatrix} = [A_{11}] [A_2] [A_4] [A_2] [A_{11}]$$

Reflection coefficient of odd mode is calculated as

$$(3.1.13) \quad \Gamma_o = \frac{A + B - C - D}{A + B + C + D}$$

Transmission coefficient of odd mode is calculated as

$$(3.1.14) \quad T_o = \frac{2}{A + B + C + D}$$

By using 3.1.8, 3.1.9, 3.1.13 and 3.1.14 Scattering parameters of the structure given in figure 3.1.1 can be calculated.

$$(3.1.15) \quad S_{11} = \frac{(\Gamma_e + \Gamma_o)}{2}$$

$$(3.1.16) \quad S_{12} = \frac{(T_e + T_o)}{2}$$

$$(3.1.17) \quad S_{13} = \frac{(T_e - T_o)}{2}$$

$$(3.1.18) \quad S_{14} = \frac{(\Gamma_e - \Gamma_o)}{2}$$

This even and odd mode analysis is used to simulate the structure (given in figure 3.1.1) in Matlab [33]. The analysis of this circuit is done by varying two parameters, one is impedance and other is length of the added shunt stub.

3.1.1.3. *Parametric study on shunt stub impedance.* The impedance of the stunt stub (Z_3 in figure 3.1.1) is varied. Impedance that are used are 0.5Ω , 0.707Ω , 1Ω , 2Ω , 3Ω and length of the stub is fixed to $\frac{\lambda}{16}$.

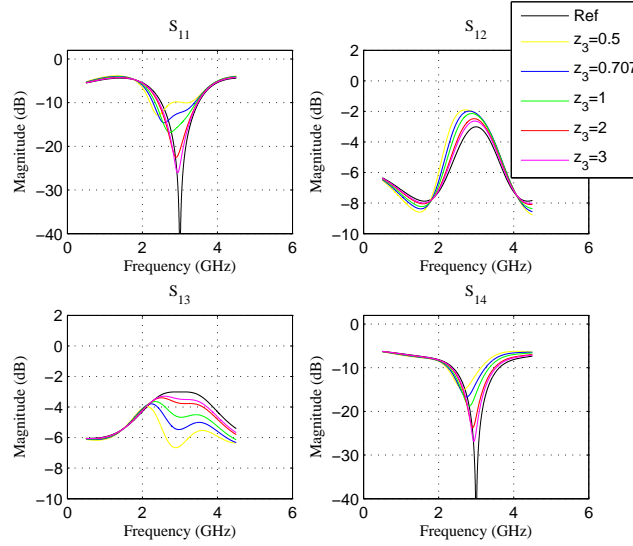


FIGURE 3.1.2. Simulation results of variable impedance for single stub

By varying the impedance of the added shunt stub it is observed that the resonance frequency is decreasing as the impedance of the added shunt stub is decreasing. This is more clearly visible from the table 1

TABLE 1. Comparison of S-parameters for different values of impedance

$Z(\Omega)$	Resonance Frequency (GHz)	$S_{11}(dB)$	$S_{12}(dB)$	$S_{13}(dB)$
0.5	2.414	-12.67	-2.488	-4.917
0.707	2.581	-14.61	-2.333	-4.606
1	2.733	-16.83	-2.30	-4.299
2	2.899	-22.51	-2.495	-3.697
3	2.939	-26.05	-2.638	-3.461
BLC	3	-40	-3.013	-3.01

3.1.1.4. *Study on variable length of shunt stub.* The impedance of added shunt stub is fixed to $Z = 1$ and length of the stub is varied from $\frac{\lambda}{32}$ to $\frac{4\lambda}{32}$.

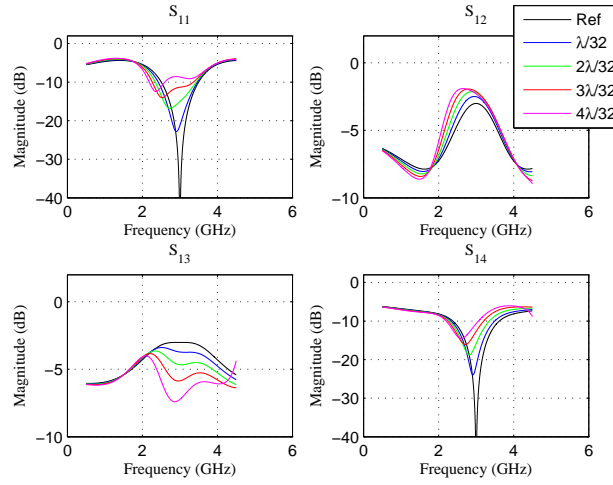


FIGURE 3.1.3. Simulation results of single stub with variable length

From figure 3.1.3 it is concluded that as the length is increasing of the added stub resonance frequency is decreasing. For $\frac{\lambda}{32}$ resonance frequency is 2.896 GHz , $\frac{2\lambda}{32}$ it is 2.717 GHz , $\frac{3\lambda}{32}$ it is 2.525 GHz , $\frac{4\lambda}{32}$ it is 2.357 GHz .

3.1.2. Double shunt stubs. Two shunt stubs are connected in the middle because of which horizontal line of branch line coupler gets divided into three equal parts as shown in figure 3.1.4.

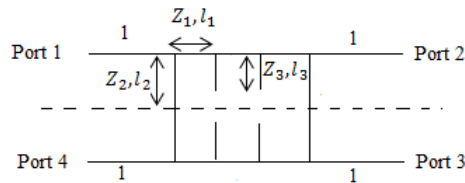


FIGURE 3.1.4. Circuit of double shunt stubs branch line coupler

Length of the original shunt stub (l_2) and impedance of original stub (Z_2) are $l_2 = \frac{\lambda}{8}$ and $Z_2 = 1$ respectively. Length of transmission line (l_1) and impedance of transmission line are $l_1 = \frac{\lambda}{12}$ and $Z_1 = \frac{1}{\sqrt{2}}$ respectively. The analysis of the circuit shown in figure 3.1.4 differ from the analysis of single stub by only 3.1.12 rest of the steps are similar. For the analysis of double stubs in the middle of branch line coupler 3.1.12 becomes

$$(3.1.19) \quad [A_3] = \begin{bmatrix} A & B \\ C & D \end{bmatrix} = [A_{11}] [A_2] [A_4] [A_2] [A_4] [A_2] [A_{11}]$$

Similar to one stub, analysis of this circuit is also done by varying two parameters one is impedance of the shunt stub and other is length of the shunt stub.

3.1.2.1. *Parametric study on shunt stubs impedance.* The impedance of the stunt stubs (Z_3 in figure 3.1.4) is varied. Impedance that are used are 0.5Ω , 0.707Ω , 1Ω , 2Ω , 3Ω and length of the stubs (Z_3 in figure 3.1.7) are fixed to $\frac{\lambda}{16}$.

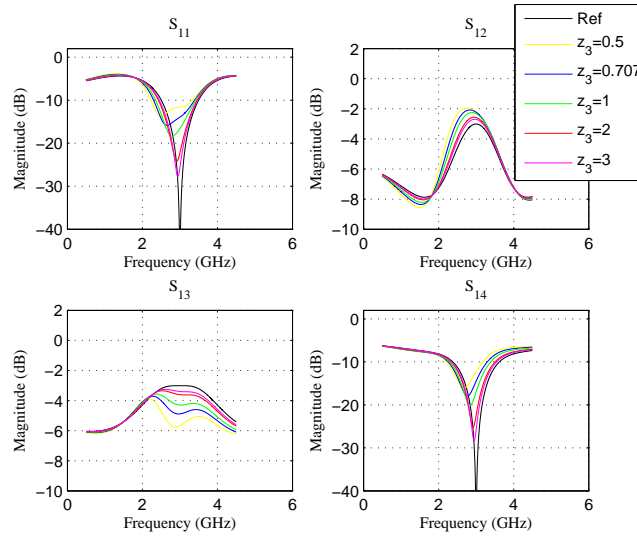


FIGURE 3.1.5. Simulation results of variable impedance for double stub

By decreasing the impedance of the two added shunt stubs it is observed that the resonance frequency is decreasing more than the first case i.e when only one stub was added in the middle. Adding stubs is leading to miniaturization because shunt stubs are increasing the capacitance of circuit which is leading to decrease in resonance frequency This is more clearly visible from the table 2

TABLE 2. Comparison of S-parameters for different values of impedance for two stubs

$Z(\Omega)$	Resonance Frequency (GHz)	$S_{11}(dB)$	$S_{12}(dB)$	$S_{13}(dB)$
0.5	2.121	-11.02	-2.818	-5.117
0.707	2.301	-12.22	-2.584	-4.908
1	2.474	-13.72	-2.4	-4.686
2	2.78	-18.12	-2.301	-4.149
3	2.872	-21.43	-2.445	-3.789
BLC	3	-40	-3.013	-3.01

3.1.2.2. *Study on variable length of shunt stubs.* The impedance of added shunt stubs is fixed to $Z = 1$ and length of the stub is varied form $\frac{\lambda}{32}$ to $\frac{4\lambda}{32}$.

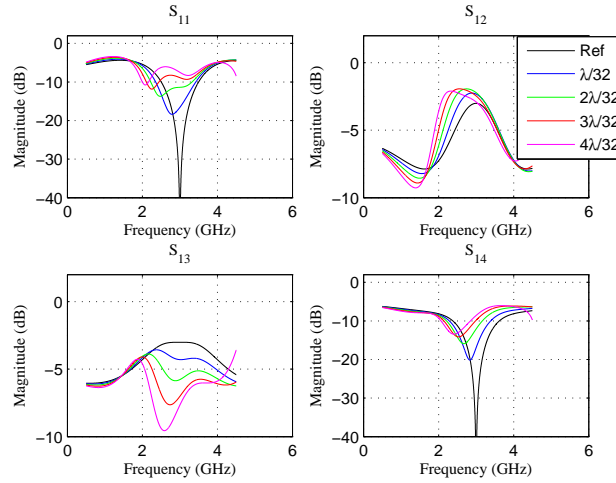


FIGURE 3.1.6. Simulation results of variable length for two stubs branch line coupler

From figure 3.1.6 it is concluded that as the length of the added stubs is increasing resonance frequency is decreasing. For $\frac{\lambda}{32}$ resonance frequency is 2.521 GHz , $\frac{2\lambda}{32}$ it is 2.01 GHz , $\frac{3\lambda}{32}$ it is 2.15 GHz , $\frac{4\lambda}{32}$ it is 2 GHz .

3.1.3. Three shunt stubs. Three shunt stubs are connected in the middle because of which horizontal line of branch line coupler gets divided into four equal parts as shown in figure 3.1.7.

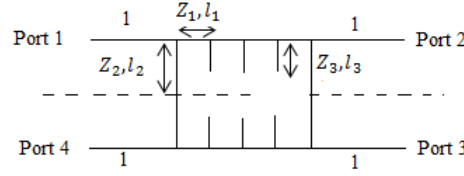


FIGURE 3.1.7. Circuit of three shunt stubs branch line coupler

Length of the original shunt stub (l_2) and impedance of original stub (Z_2) are $l_2 = \frac{\lambda}{8}$ and $Z_2 = 1$ respectively. Length of transmission line (l_1) and impedance of transmission line are $l_1 = \frac{\lambda}{16}$ and $Z_1 = \frac{1}{\sqrt{2}}$ respectively. The analysis of the circuit shown in figure 3.1.7 differ from the analysis of single stub by only 3.1.12 rest of the steps are similar. For the analysis of three stubs in the middle of branch line coupler 3.1.12 becomes

$$(3.1.20) \quad [A_3] = \begin{bmatrix} A & B \\ C & D \end{bmatrix} = [A_{11}] [A_2] [A_4] [A_2] [A_4] [A_2] [A_4] [A_2] [A_{11}]$$

Analysis of this circuit is also done by varying same parameters impedance of the shunt stub and length of the shunt stub.

3.1.3.1. *Parametric study on shunt stubs impedance.* The impedance of the stunt stubs (Z_3 in figure 3.1.7) is varied. Impedance that are used are 0.5Ω , 0.707Ω , 1Ω , 2Ω , 3Ω and length of the stubs (l_3 in figure 3.1.7) are fixed to $\frac{\lambda}{16}$.

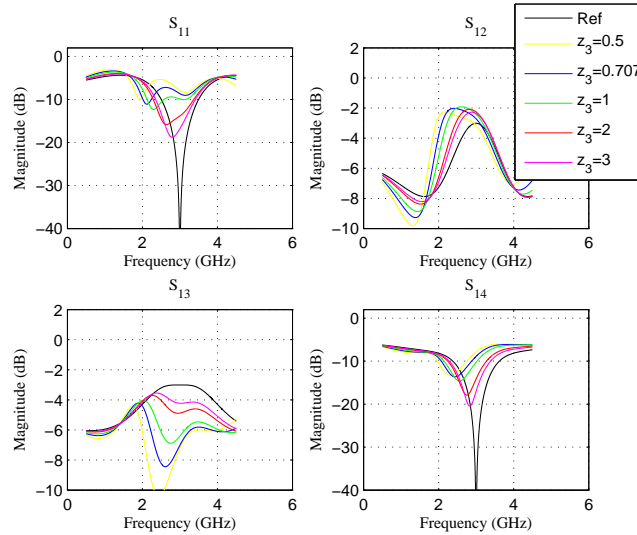


FIGURE 3.1.8. Simulation results of variable impedance for three stubs

By decreasing the impedance of the added shunt stubs it is observed that the resonance frequency is decreasing more than the second case i.e when two stubs are added in the middle. This is more clearly visible from the table 3

TABLE 3. Comparison of S-parameters for different values of impedance for three stubs

$Z(\Omega)$	Resonance Frequency (GHz)	$S_{11}(dB)$	$S_{12}(dB)$	$S_{13}(dB)$
0.5	1.928	-10.1	-3.08	-5.271
0.707	2.1	-11.07	-2.9	-4.976
1	2.297	-12.32	-2.571	-4.882
2	2.628	-15.81	-2.315	-4.39
3	2.789	-18.77	-2.33	-4.059
BLC	3	-40	-3.013	-3.01

3.1.3.2. *Study on variable length of shunt stubs.* The impedance of added shunt stubs is fixed to $Z = 1$ and length of the stubs is varied form $\frac{\lambda}{32}$ to $\frac{4\lambda}{32}$.

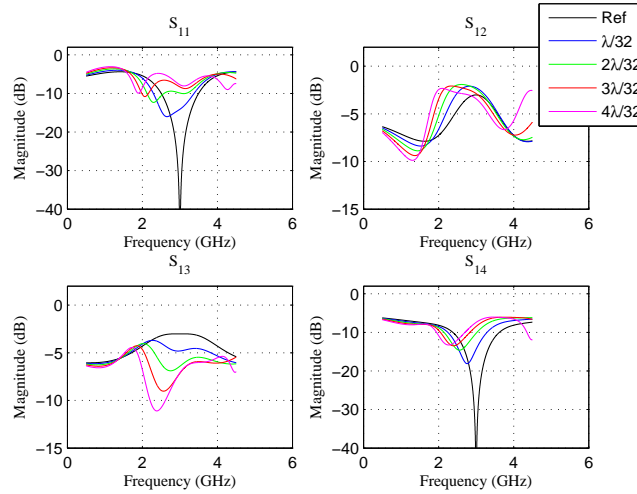


FIGURE 3.1.9. Simulation results of variable length for three stubs branch line coupler

From figure 3.1.9 it is concluded that as the lengths of the added stubs are increasing resonance frequency is decreasing. For $\frac{\lambda}{32}$ resonance frequency is 2.644 GHz , $\frac{2\lambda}{32}$ it is 2.287 GHz , $\frac{3\lambda}{32}$ it is 2.073 GHz , $\frac{4\lambda}{32}$ it is 1.89 GHz .

3.1.4. Five shunt stubs. Five shunt stubs are connected in the middle because of which horizontal line of branch line coupler gets divided into six equal parts as shown in figure 3.1.10.

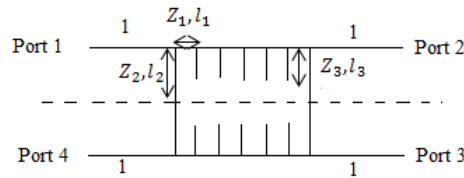


FIGURE 3.1.10. Circuit of five shunt stubs branch line coupler

Length of the original shunt stub (l_2) and impedance of original stub (Z_2) are $l_2 = \frac{\lambda}{8}$ and $Z_2 = 1$ respectively. Length of transmission line (l_1) and impedance of transmission line are $l_1 = \frac{\lambda}{24}$ and $Z_1 = \frac{1}{\sqrt{2}}$ respectively. The analysis of the circuit shown in figure 3.1.10 differ from the analysis of single stub by only 3.1.12 rest of the steps are similar. For the analysis of five stubs in the middle of branch line coupler 3.1.12 becomes

$$(3.1.21) \quad [A_3] = \begin{bmatrix} A & B \\ C & D \end{bmatrix} = [A_{11}] [A_2] [A_4] [A_2] [A_4] [A_2] [A_4] [A_2] [A_4] [A_2] [A_{11}]$$

Analysis of this circuit is also done by varying same parameters impedance of the shunt stub and length of the shunt stub.

3.1.4.1. *Parametric study on shunt stubs impedance.* The impedance of the stunt stubs (Z_3 in figure 3.1.10) is varied. Impedance that are used are 0.5Ω , 0.707Ω , 1Ω , 2Ω , 3Ω and length of the stubs are fixed to $\frac{\lambda}{16}$.

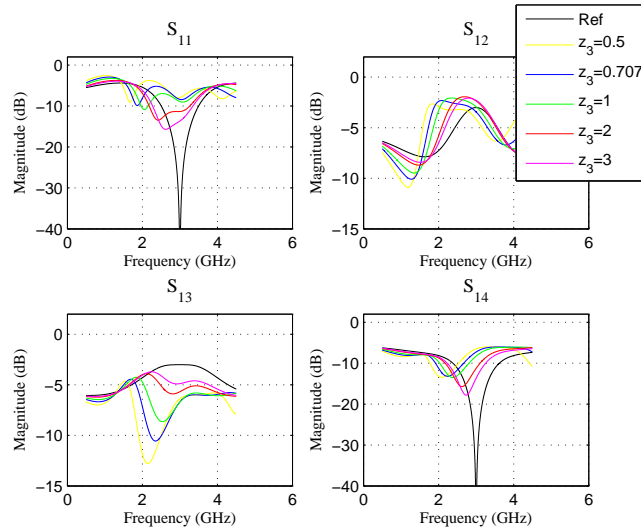


FIGURE 3.1.11. Simulation results of variable impedance for five stubs

By decreasing the impedance of the added shunt stubs it can be observed that the resonance frequency is decreasing more than the third case i.e when three stubs are added in the middle. This is more clearly visible from the table 4

TABLE 4. Comparison of S-parameters for different values of impedance for five stubs

$Z(\Omega)$	Resonance Frequency (GHz)	$S_{11}(dB)$	$S_{12}(dB)$	$S_{13}(dB)$
0.5	1.671	-9.08	-3.843	-5.458
0.707	1.862	-9.88	-3.153	-5.295
1	2.052	-10.58	-2.867	-5.134
2	2.424	-13.32	-2.394	-4.746
3	2.619	-15.69	-2.282	-4.441
BLC	3	-40	-3.013	-3.01

3.1.4.2. *Study on variable length of shunt stubs.* The impedance of added shunt stubs is fixed to $Z = 1$ and length of the stubs is varied form $\frac{\lambda}{32}$ to $\frac{4\lambda}{32}$.

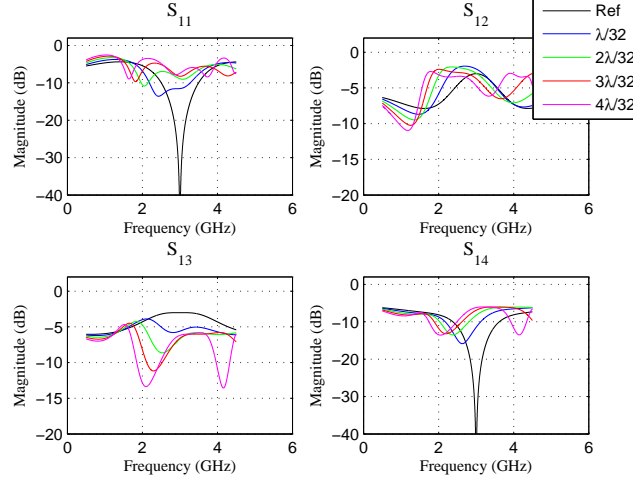


FIGURE 3.1.12. Simulation results of variable length for five stubs branch line coupler

From figure 3.1.12 it can be concluded that as the length is increasing of the added stubs resonance frequency is decreasing. For $\frac{\lambda}{32}$ resonance frequency is 2.43 GHz , $\frac{2\lambda}{32}$ it is 2.049 GHz , $\frac{3\lambda}{32}$ it is 1.814 GHz , $\frac{4\lambda}{32}$ it is 1.643 GHz .

3.2. Stubs in the vertical branches

To come up with miniaturized structure of branch line coupler the same analysis is performed with vertical branches of the coupler.

3.2.1. Two shunt stubs. Firstly two shunt stubs are connected in vertical branch of branch line coupler and there are no stubs in the horizontal line of branch line coupler. Circuit of branch line coupler with two vertical stubs are shown in figure 3.2.1.

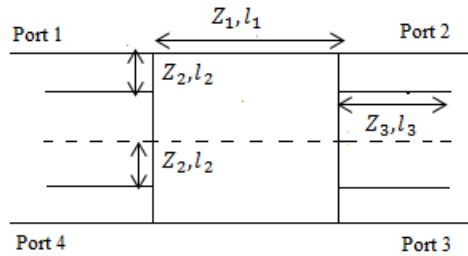


FIGURE 3.2.1. Circuit of two vertical stubs branch line coupler

Length of the original shunt stub (l_2) and impedance of original stub (Z_2) are $l_2 = \frac{\lambda}{16}$ and $Z_2 = 1$ respectively. Length of transmission line (l_1) and impedance of transmission line are

$l_1 = \frac{\lambda}{4}$ and $Z_1 = \frac{1}{\sqrt{2}}$ respectively. Analysis of the circuit given in figure 3.2.1 is done to find out the optimum length l_3 and impedance Z_2 of added stubs.

3.2.1.1. *Even mode analysis.* For calculating the the even mode reflection and transmission coefficients, multiplication of ABCD matrix of all the cascaded elements is done.

Impedance of line l_2

$$(3.2.1) \quad Z_{inl1} = -jZ_2 \cot(\beta l_2)$$

Impedance of added stub of length l_3

$$(3.2.2) \quad Z_{inl3} = -jZ_3 \cot(\beta l_3)$$

These two stubs are in parallel with each other

$$(3.2.3) \quad Z_p = \frac{Z_{inl1} Z_{inl3}}{Z_{inl1} + Z_{inl3}}$$

This parallel combination is acting as a load to l_2

$$(3.2.4) \quad Z_{in1} = Z_2 \frac{Z_p + (jZ_2 \tan(\beta l_2))}{Z_2 + (jZ_p \tan(\beta l_2))}$$

ABCD matrix of original shunt stub with a vertical stub

$$(3.2.5) \quad [A_1] = \begin{bmatrix} 1 & 0 \\ \frac{1}{Z_{int1}} & 1 \end{bmatrix}$$

ABCD matrix of transmission line

$$(3.2.6) \quad [A_2] = \begin{bmatrix} \cos(\beta l_1) & jZ_1 \sin(\beta l_1) \\ j\frac{1}{Z_1} \sin(\beta l_1) & \cos(\beta l_1) \end{bmatrix}$$

ABCD matrix of even mode cascaded elements

$$(3.2.7) \quad [A_3] = \begin{bmatrix} A & B \\ C & D \end{bmatrix} = [A_1] [A_2] [A_1]$$

Reflection coefficient of even mode can be calculated as

$$(3.2.8) \quad \Gamma_e = \frac{A + B - C - D}{A + B + C + D}$$

Transmission coefficient of even mode can be calculated as

$$(3.2.9) \quad T_e = \frac{2}{A + B + C + D}$$

The analysis of this circuit is done by varying the same parameters that are impedance of the shunt stub and length of the shunt stub.

3.2.1.2. *Odd mode analysis.* Similar steps are followed for calculating reflection and transmission coefficients for odd case.

$$(3.2.10) \quad Z_{inlo} = jZ_2 \tan(\beta l_2)$$

by using 3.2.2

$$(3.2.11) \quad Z_{p2} = \frac{Z_{inlo} Z_{inl3}}{Z_{inlo} + Z_{inl3}}$$

This parallel combination is acting as a load to l_2

$$(3.2.12) \quad Z_{in2} = Z_2 \frac{Z_{p2} + (jZ_2 \tan(\beta l_2))}{Z_2 + (jZ_{p2} \tan(\beta l_2))}$$

This is the ABCD matrix of original shunt stub of length l_2

$$(3.2.13) \quad [A_{11}] = \begin{bmatrix} 1 & 0 \\ \frac{1}{Z_{in2}} & 1 \end{bmatrix}$$

ABCD matrix of transmission line is given in 3.2.6, ABCD matrix of odd mode cascaded elements

$$(3.2.14) \quad [A_3] = \begin{bmatrix} A & B \\ C & D \end{bmatrix} = [A_{11}] [A_2] [A_{11}]$$

Reflection coefficient of odd mode can be calculated as

$$(3.2.15) \quad \Gamma_o = \frac{A + B - C - D}{A + B + C + D}$$

Transmission coefficient of odd mode can be calculated as

$$(3.2.16) \quad T_o = \frac{2}{A + B + C + D}$$

By using 3.2.8, 3.2.9, 3.2.15 and 3.2.16 Scattering parameters of the structure given in figure 3.2.1 can be calculated.

$$(3.2.17) \quad S_{11} = \frac{(\Gamma_e + \Gamma_o)}{2}$$

$$(3.2.18) \quad S_{12} = \frac{(T_e + T_o)}{2}$$

$$(3.2.19) \quad S_{13} = \frac{(T_e - T_o)}{2}$$

$$(3.2.20) \quad S_{14} = \frac{(\Gamma_e - \Gamma_o)}{2}$$

This even and odd mode analysis is used to simulate the structure (given in figure 3.2.1) in Matlab [33]. The analysis of this circuit is done by varying two parameters, one is impedance and other is length of the added shunt stub.

3.2.1.3. *Parametric study on shunt stubs impedance.* The impedance of the stunt stubs (Z_3 in figure 3.2.1) is varied. Impedance that are used are 0.5Ω , 0.707Ω , 1Ω , 2Ω , 3Ω and length of the stubs (Z_3 in figure 3.2.1) are fixed to $\frac{\lambda}{16}$.

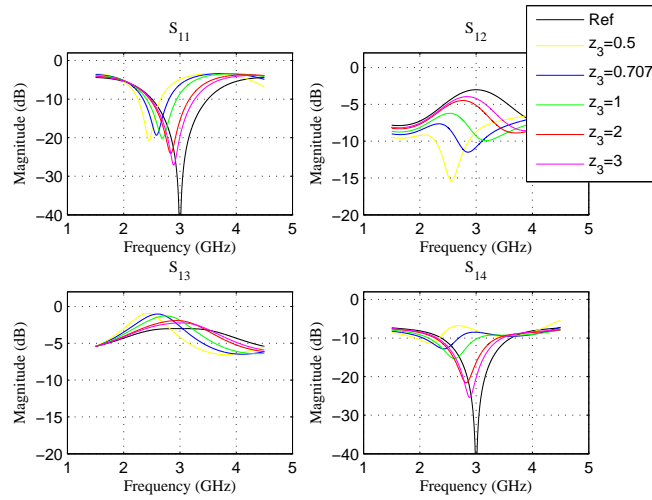


FIGURE 3.2.2. Simulation results of variable impedance for two vertical stubs

By decreasing the impedance of the two added shunt stubs it can be observed that the resonance frequency is decreasing. This is more clearly visible from the table 5

TABLE 5. Comparison of S-parameters for different values of impedance for two vertical stubs

$Z(\Omega)$	Resonance Frequency (GHz)	$S_{11}(dB)$	$S_{12}(dB)$	$S_{13}(dB)$
0.5	2.488	-19	-14.37	-1.032
0.707	2.586	-19.37	-8.94	-1.027
1	2.691	-20.13	-6.634	-1.306
2	2.835	-23.98	-4.534	-1.958
3	2.889	-27.09	-3.969	-2.26
BLC	3	-40	-3.013	-3.01

3.2.1.4. *Study on variable length of shunt stubs.* The impedance of added shunt stubs is fixed to $Z = 1$ and length of the stubs is varied form $\frac{\lambda}{32}$ to $\frac{4\lambda}{32}$.

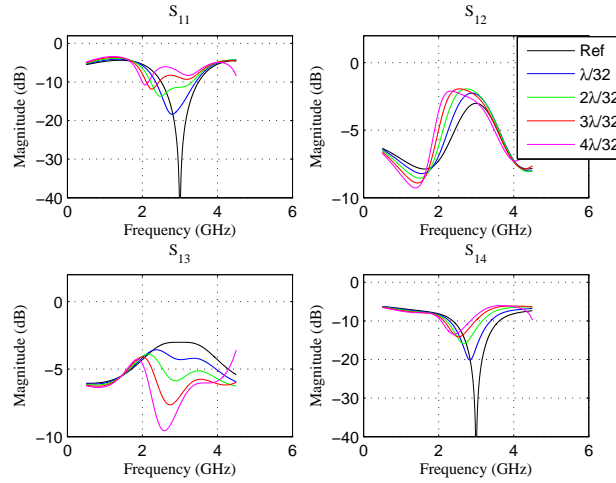


FIGURE 3.2.3. Simulation results of variable length for two vertical stubs branch line coupler

From figure 3.2.3 it is concluded that as the length of the added stubs is increasing resonance frequency is decreasing. For $\frac{\lambda}{32}$ resonance frequency is 2.839 GHz , $\frac{2\lambda}{32}$ it is 2.687 GHz , $\frac{3\lambda}{32}$ it is 2.543 GHz , $\frac{4\lambda}{32}$ it is 2.4 GHz .

3.2.2. Four shunt stubs. Four shunt stubs are connected in vertical branch of branch line coupler and there are no stubs in the horizontal line of branch line coupler. Circuit of branch line coupler with four vertical stubs are shown in figure 3.2.4

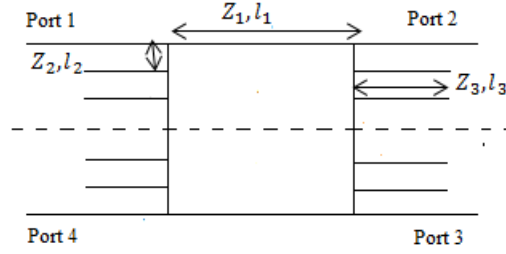


FIGURE 3.2.4. Circuit of branch line coupler with four vertical stubs

Length of the original shunt stub (l_2) and impedance of original stub (Z_2) are $l_2 = \frac{\lambda}{24}$ and $Z_2 = 1$ respectively. Length of transmission line (l_1) and impedance of transmission line are $l_1 = \frac{\lambda}{4}$ and $Z_1 = \frac{1}{\sqrt{2}}$ respectively. Analysis of the circuit given in figure 3.2.4 is done to find out the optimum length l_3 and impedance Z_2 of added stubs.

3.2.2.1. *Even mode analysis.* For calculating the the even mode reflection and transmission coefficients, multiplication of ABCD matrix of all the cascaded elements is done.

Impedance of line l_2

$$(3.2.21) \quad Z_{inl2} = -jZ_2 \cot(\beta l_2)$$

Impedance of added stub of length l_3

$$(3.2.22) \quad Z_{inl3} = -jZ_3 \cot(\beta l_3)$$

These two stubs are in parallel with each other

$$(3.2.23) \quad Z_{pe} = \frac{Z_{inl2} Z_{inl3}}{Z_{inl2} + Z_{inl3}}$$

This parallel combination is acting as a load to l_2

$$(3.2.24) \quad Z_{in1e} = Z_2 \frac{Z_{pe} + (jZ_2 \tan(\beta l_2))}{Z_2 + (jZ_{pe} \tan(\beta l_2))}$$

These two stubs are in parallel with each other

$$(3.2.25) \quad Z_p = \frac{Z_{in1e} Z_{inl3}}{Z_{in1e} + Z_{inl3}}$$

This parallel combination is acting as a load to l_2

$$(3.2.26) \quad Z_{in1} = Z_2 \frac{Z_p + (jZ_2 \tan(\beta l_2))}{Z_2 + (jZ_p \tan(\beta l_2))}$$

ABCD matrix of original shunt stub with a vertical stub

$$(3.2.27) \quad [A_1] = \begin{bmatrix} 1 & 0 \\ \frac{1}{Z_{int1}} & 1 \end{bmatrix}$$

ABCD matrix of transmission line

$$(3.2.28) \quad [A_2] = \begin{bmatrix} \cos(\beta l_1) & jZ_1 \sin(\beta l_1) \\ j\frac{1}{Z_1} \sin(\beta l_1) & \cos(\beta l_1) \end{bmatrix}$$

ABCD matrix of even mode cascaded elements

$$(3.2.29) \quad [A_3] = \begin{bmatrix} A & B \\ C & D \end{bmatrix} = [A_1] [A_2] [A_1]$$

Reflection coefficient of even mode can be calculated as

$$(3.2.30) \quad \Gamma_e = \frac{A + B - C - D}{A + B + C + D}$$

Transmission coefficient of even mode can be calculated as

$$(3.2.31) \quad T_e = \frac{2}{A + B + C + D}$$

3.2.2.2. *Odd mode analysis.* Similar steps are followed for calculating reflection and transmission coefficients for odd case.

$$(3.2.32) \quad Z_{inlo} = jZ_2 \tan(\beta l_2)$$

by using 3.2.22

$$(3.2.33) \quad Z_{po2} = \frac{Z_{inlo} Z_{inl3}}{Z_{inlo} + Z_{inl3}}$$

This parallel combination is acting as a load to l_2

$$(3.2.34) \quad Z_{in2o} = Z_2 \frac{Z_{p2} + (jZ_2 \tan(\beta l_2))}{Z_2 + (jZ_{p2} \tan(\beta l_2))}$$

$$(3.2.35) \quad Z_{p2} = \frac{Z_{in2o} Z_{inl3}}{Z_{in2o} + Z_{inl3}}$$

This parallel combination is acting as a load to l_2

$$(3.2.36) \quad Z_{in2o} = Z_2 \frac{Z_{p2} + (jZ_2 \tan(\beta l_2))}{Z_2 + (jZ_{p2} \tan(\beta l_2))}$$

Now

$$(3.2.37) \quad [A_{11}] = \begin{bmatrix} 1 & 0 \\ \frac{1}{Z_{in2}} & 1 \end{bmatrix}$$

ABCD matrix of transmission line is given in 3.2.28, ABCD matrix of odd mode cascaded elements

$$(3.2.38) \quad [A_3] = \begin{bmatrix} A & B \\ C & D \end{bmatrix} = [A_{11}] [A_2] [A_{11}]$$

Reflection coefficient of odd mode can be calculated as

$$(3.2.39) \quad \Gamma_o = \frac{A + B - C - D}{A + B + C + D}$$

Transmission coefficient of odd mode can be calculated as

$$(3.2.40) \quad T_o = \frac{2}{A + B + C + D}$$

By using 3.2.30, 3.2.31, 3.2.39 and 3.2.40 Scattering parameters of the structure given in figure 3.2.4 can be calculated.

$$(3.2.41) \quad S_{11} = \frac{(\Gamma_e + \Gamma_o)}{2}$$

$$(3.2.42) \quad S_{12} = \frac{(T_e + T_o)}{2}$$

$$(3.2.43) \quad S_{13} = \frac{(T_e - T_o)}{2}$$

$$(3.2.44) \quad S_{14} = \frac{(\Gamma_e - \Gamma_o)}{2}$$

This even and odd mode analysis is used to simulate the structure (given in figure 3.2.4) in Matlab [33]. The analysis of this circuit is done by varying two parameters, one is impedance and other is length of the added shunt stub.

3.2.2.3. *Parametric study on shunt stubs impedance.* The impedance of the stunt stubs (Z_3 in figure 3.2.4) is varied. Impedance that are used are 0.5Ω , 0.707Ω , 1Ω , 2Ω , 3Ω and length of the stubs (Z_3 in figure 3.2.4) are fixed to $\frac{\lambda}{16}$.

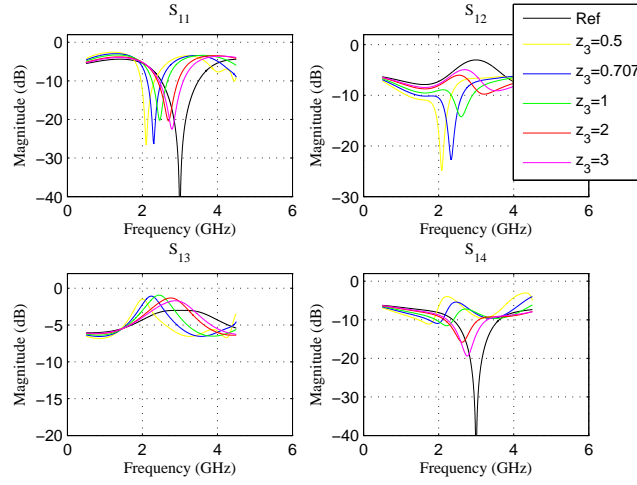


FIGURE 3.2.5. Simulation results of variable impedance for four vertical stubs

By decreasing the impedance of the two added shunt stubs it is observed that the resonance frequency is decreasing more than the first case i.e when two stubs are added in the middle of vertical branch. This is more clearly visible from the table 6

TABLE 6. Comparison of S-parameters for different values of impedance for four vertical stubs

$Z(\Omega)$	Resonance Frequency (GHz)	$S_{11}(dB)$	$S_{12}(dB)$	$S_{13}(dB)$
0.5	2.095	-26.28	-24	-1.811
0.707	2.296	-26.15	-20.83	-1.165
1	2.46	-20.24	-9.19	-0.9433
2	2.694	-20.38	-6.368	-1.36
3	2.784	-22.53	-5.03	-1.748
BLC	3	-40	-3.013	-3.01

3.2.2.4. *Study on variable length of shunt stubs.* The impedance of added shunt stubs is fixed to $Z = 1$ and length of the stub is varied from $\frac{\lambda}{32}$ to $\frac{4\lambda}{32}$.

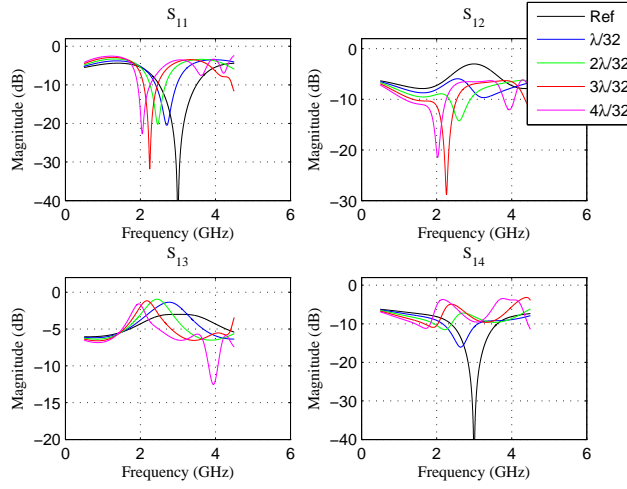


FIGURE 3.2.6. Simulation results of variable length for four vertical stubs branch line coupler

From figure 3.2.6 it is concluded that as the length of the added stubs is increasing resonance frequency is decreasing. For $\frac{\lambda}{32}$ resonance frequency is 2.718 GHz , $\frac{2\lambda}{32}$ it is 2.463 GHz , $\frac{3\lambda}{32}$ it is 2.246 GHz , $\frac{4\lambda}{32}$ it is 2.048 GHz .

3.2.3. Five shunt stubs. Five shunt stubs are connected in vertical branch of branch line coupler and there are no stubs in the horizontal line. Circuit of branch line coupler with five vertical stubs are shown in figure 3.2.7

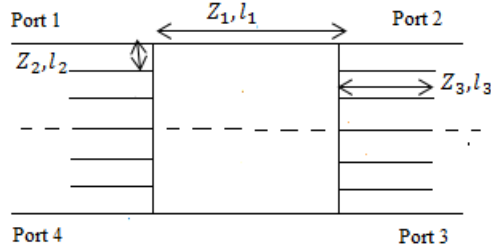


FIGURE 3.2.7. Circuit of branch line coupler with five vertical stubs

Length of the original shunt stub (l_2) and impedance of original stub (Z_2) are $l_2 = \frac{\lambda}{24}$ and $Z_2 = 1$ respectively. Length of transmission line (l_1) and impedance of transmission line are $l_1 = \frac{\lambda}{4}$ and $Z_1 = \frac{1}{\sqrt{2}}$ respectively. Analysis of the circuit given in figure 3.2.7 is done to find out the optimum length l_3 and impedance Z_2 of added stubs.

The mathematical analysis of five stubs in the vertical branch of branch line coupler is different from all the cases discussed above. For even and odd case the middle stub gets divided into two half by horizontal symmetry line.

3.2.3.1. *Even mode analysis.*

$$(3.2.45) \quad Z_{inl1} = -jZ_2 \cot(\beta l_2)$$

Impedance of added stub of length l_3

$$(3.2.46) \quad Z_{inl3} = -jZ_3 \cot(\beta l_3)$$

Characteristic impedance of middle stub acting as a load to l_2

$$(3.2.47) \quad Z_{ins} = Z_2 \frac{2Z_{inl3} + (jZ_2 \tan(\beta l_2))}{Z_2 + (j2Z_{inl3} \tan(\beta l_2))}$$

now

$$(3.2.48) \quad Z_{pe} = \frac{Z_{ins} Z_{inl3}}{Z_{ins} + Z_{inl3}}$$

$$(3.2.49) \quad Z_{inle} = Z_2 \frac{Z_{pe} + (jZ_2 \tan(\beta l_2))}{Z_2 + (jZ_{pe} \tan(\beta l_2))}$$

$$(3.2.50) \quad Z_p = \frac{Z_{inle} Z_{inl3}}{Z_{inle} + Z_{inl3}}$$

$$(3.2.51) \quad Z_{in1} = Z_2 \frac{Z_p + (jZ_2 \tan(\beta l_2))}{Z_2 + (jZ_p \tan(\beta l_2))}$$

Matrix $[A_1]$ is similar to 3.2.27 and Matrix $[A_2]$ is similar to 3.2.28. Reflection and transmission coefficients are found out by using 3.2.30 and 3.2.31

3.2.3.2. *Odd mode analysis.* As there is no point in connecting the stub in the middle of vertical line of the coupler because it will be short circuited in odd mode, so analysis of odd mode is same as the odd mode of branch line coupler with four vertical stubs.

The result of the five vertical stubs integrated with five horizontal stubs is given in figure 3.4.8

3.3. Stubs in vertical and horizontal branches

Combined effect of adding the stubs in horizontal and vertical branches of branch line coupler, on the S-parameters of the coupler is analyzed in this section to select the optimum values of the stubs length and impedance

3.3.1. Four vertical stubs with one horizontal stub. Circuit of branch line coupler with four vertical stubs with one horizontal stubs is shown in figure 3.3.1

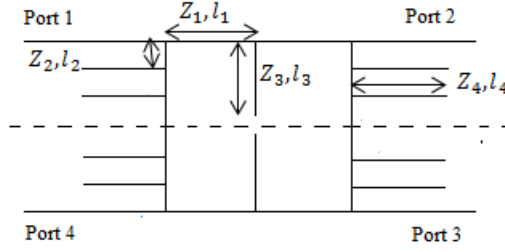


FIGURE 3.3.1. Circuit of branch line coupler with four stubs in vertical branch and one stub in horizontal branch

Length of the original shunt stub (l_2) and impedance of original stub (Z_2) are $l_2 = \frac{\lambda}{24}$ and $Z_2 = 1$ respectively. Length of transmission line (l_1) and impedance of transmission line are $l_1 = \frac{\lambda}{8}$ and $Z_1 = \frac{1}{\sqrt{2}}$ respectively. Length l_4 and impedance Z_4 of of vertical stubs are fixed to $l_4 = \frac{\lambda}{16}$ and $Z_4 = 1$ respectively. Analysis of the circuit given in figure 3.3.1 is done to find out the optimum length l_3 and impedance Z_2 of added stubs.

3.3.1.1. *Parametric study on shunt stubs impedance.* The impedance of the stunt stubs (Z_3 in figure 3.2.4) is varied. Impedance that are used are 0.5Ω , 0.707Ω , 1Ω , 2Ω , 3Ω and length of the stubs (Z_3 in figure 3.2.4) are fixed to $\frac{\lambda}{16}$.

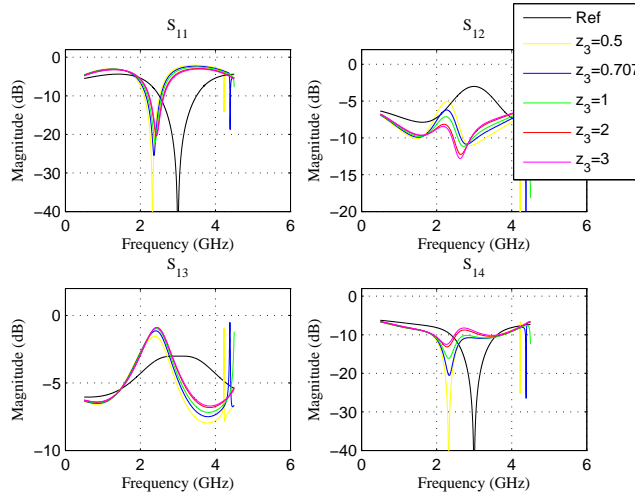


FIGURE 3.3.2. Simulation results of branch line coupler with four stubs in vertical branch and one in horizontal branch

By decreasing the impedance of the horizontally added shunt stub it can be observed that the resonance frequency is decreasing. This is more clearly visible from the table 7

TABLE 7. Comparison of S-parameters of branch line coupler with four stubs in vertical branch and one in horizontal branch

$Z(\Omega)$	Resonance Frequency (GHz)	$S_{11}(dB)$	$S_{12}(dB)$	$S_{13}(dB)$
0.5	2.32	-37.87	-5.102	-1.605
0.707	2.361	-25.48	-6.476	-1.177
1	2.39	-22.12	-7.735	-0.9882
2	2.426	-20.41	-9.668	-0.8919
3	2.437	-20.21	-10.42	-0.89
BLC	3	-40	-3.013	-3.01

3.3.1.2. *Study on variable length of shunt stubs.* The impedance of all added shunt stub is fixed to $Z = 1$ and length of the stub that are added vertically is $\frac{2\lambda}{32}$. Length of horizontally added stub is varied form $\frac{\lambda}{32}$ to $\frac{4\lambda}{32}$.

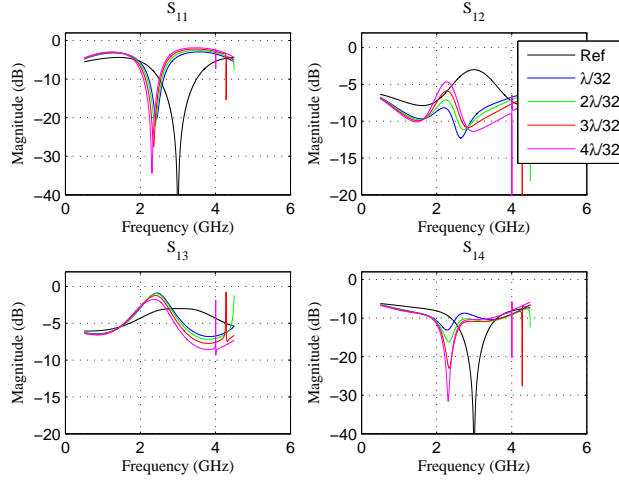


FIGURE 3.3.3. Simulation results of variable length for four vertical stubs and one horizontal stub branch line coupler

From figure 3.3.3 it is concluded that as the length of the added stubs is increasing resonance frequency is decreasing. For $\frac{\lambda}{32}$ resonance frequency is 2.427 GHz , $\frac{2\lambda}{32}$ it is 2.392 GHz , $\frac{3\lambda}{32}$ it is 2.351 GHz , $\frac{4\lambda}{32}$ it is 2.308 GHz .

Similarly stubs are added in the horizontal branch one by one with four stubs in the vertical branch but in this report last case is shown when four vertical stubs are added with five stubs in vertical branch

3.3.2. Four vertical stubs with five horizontal stub. Five stubs are connected in the horizontal branch of the coupler and four stubs are added in the vertical branch of the coupler. Circuit diagram of branch line coupler with five stubs in horizontal branches and four stubs in vertical branches is shown in figure 3.3.4

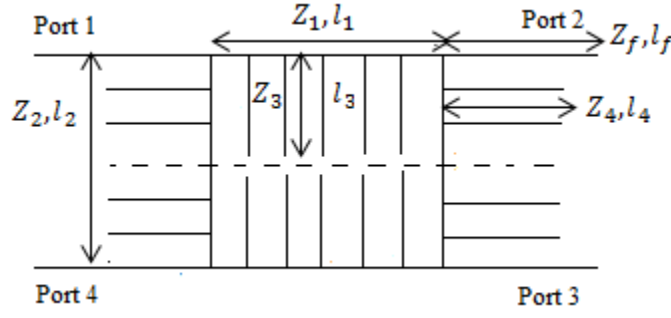


FIGURE 3.3.4. Circuit diagram of miniaturized branch line coupler with five stubs in horizontal branches and four stubs in vertical branches

Length of the original shunt stub (l_2) and impedance of original stub (Z_2) are $l_2 = \frac{\lambda}{4}$ and $Z_2 = 1$ respectively. Length of transmission line (l_1) and impedance of transmission line are $l_1 = \frac{\lambda}{4}$ and $Z_1 = \frac{1}{\sqrt{2}}$ respectively. Length l_4 and impedance Z_4 of vertical stubs are fixed to $l_4 = \frac{\lambda}{16}$ and $Z_4 = 1$ respectively. Analysis of the circuit given in figure 3.3.4 is done to find out the optimum length l_3 and impedance Z_3 of added stubs.

3.3.2.1. *Parametric study on shunt stubs impedance.* The impedance of the stunt stubs (Z_3 in figure 3.3.4) is varied. Impedance that are used are 0.5Ω , 0.707Ω , 1Ω , 2Ω , 3Ω and length of the stubs (l_3 in figure 3.3.4) are fixed to $\frac{\lambda}{16}$.

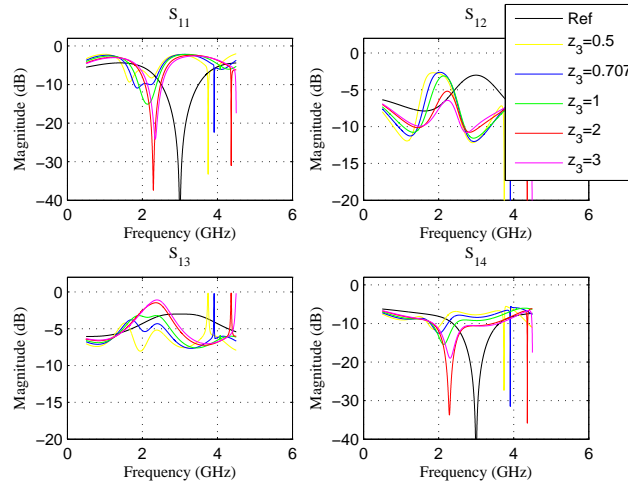


FIGURE 3.3.5. Simulation results of branch line coupler with four stubs in vertical branch and five in horizontal branch

By decreasing the impedance of the horizontally added shunt stub it can be observed that the resonance frequency is decreasing. This is more clearly visible from the table 8

TABLE 8. Comparison of S-parameters of branch line coupler with four stubs in vertical branch and five in horizontal branch

$Z(\Omega)$	Resonance Frequency (GHz)	$S_{12}(dB)$	$S_{13}(dB)$
0.5	1.655	-3.548	-4.918
0.707	1.864	-3.18	-4.415
1	2.137	-3.111	-3.451
2	2.291	-5.295	-1.525
3	2.344	-6.779	-1.122
BLC	3	-3.013	-3.01

From table 8 it can be concluded that impedance values 0.5 , 0.707 and 1 are appropriate to use but reflection coefficient of 0.5 , 0.707 and 1 are -9.34 dB, -10.92 dB, -15.08dB respectively. So optimum value of impedance is 1 (normalized with 50 Ω) for equal power division at output ports with less reflections.

3.3.2.2. *Study on variable length of shunt stubs.* The impedance of all added shunt stub is fixed to $Z = 1$ and length of the stub that are added vertically is $\frac{2\lambda}{32}$. Length of horizontally added stub is varied form $\frac{\lambda}{32}$ to $\frac{4\lambda}{32}$.

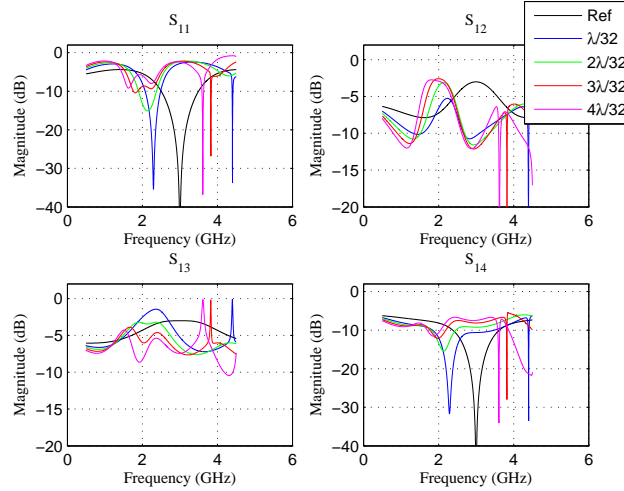


FIGURE 3.3.6. Simulation results of variable length for four vertical stubs and five horizontal stub branch line coupler

From figure 3.3.6 it is concluded that as the length of the added stubs is increasing resonance frequency is decreasing. When length is $\frac{\lambda}{32}$ magnitude of S_{12} and S_{13} are -5.373 dB and -1.495 dB respectively at 2.294 GHz frequency. At $\frac{2\lambda}{32}$ length magnitude of S_{12} and S_{13} are -3.11 dB and -3.451 dB respectively at 2.137 GHz. At length $\frac{3\lambda}{32}$ magnitude of S_{12} and S_{13} are -3.348 dB and -4.49 dB respectively at 1.802 GHz and when length is $\frac{4\lambda}{32}$ magnitude of S_{12} and S_{13} are -3.61 dB and -4.962 dB respectively at 1.627 GHz frequency

From figure 3.3.6 optimum length of stubs are $\frac{\lambda}{16}$ because only at this length power is equal dividing between two output ports

3.4. Miniaturized branch line coupler

In the last section, optimum values of length and impedance of stubs for the horizontal and vertical cases are obtained and that are $l = \frac{\lambda}{16}$ and $Z = 1$ (normalized by 50Ω) respectively. This combination of length and width has S_{12} and S_{13} closer to -3 dB . In this section by using the optimum values of length and impedance the miniaturized structure is designed in Fullwave EM simulator (CST microwave studio) [32].

3.4.1. Branch line coupler with four stubs on vertical branches and five stubs on horizontal branch. Branch line coupler with four stubs on vertical branches and five stubs on horizontal branch of coupler is designed and analyzed in this section

The impedance of all the added stubs is one (normalized by 50Ω) and length is $\frac{\lambda}{16}$. Matlab simulation results are shown in figure 3.4.1

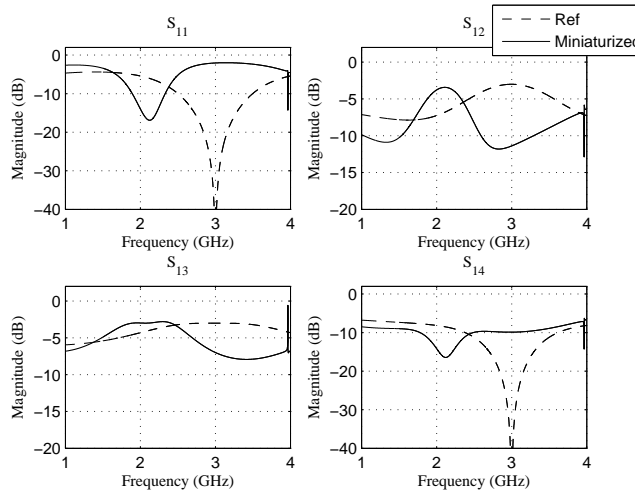


FIGURE 3.4.1. Matlab simulation result of comparison of miniaturized branch line coupler with conventional branch line coupler

In figure 3.4.1 comparison of modified branch line coupler (branch line coupler with five horizontal stubs and four vertical stubs) with conventional branch line coupler operating at 3 GHz is shown. The frequency of miniaturized branch line coupler is 2.137 GHz and conventional branch line coupler is 3 GHz . By adding stubs the frequency shifted from 3 GHz to 2.137 GHz , this means that branch line coupler dimensions are unchanged for 2.137 GHz , where as in the normal scenario (branch line coupler with no stubs) dimension should have increased because at lower frequency λ increases. Because of the usage of stubs in the branch line coupler structure dimension of branch line coupler operating at 3 GHz frequency can be used at branch line coupler operating at 2.137 GHz

3.4.1.1. CST simulation results of branch line coupler with four vertical stubs. The miniaturized branch line coupler is designed in Fullwave EM simulator (CST microwave studio) [32]. The structure is placed on the material RT-Duroid 5880 which has properties that are mentioned in table 9.

TABLE 9. Properties of RT-Duroid 5880

$t_c(mm)$	$h(mm)$	ϵ_r	μ_r
0.035	0.508	2.2	1
Thickness of substrate and conductor	Height of substrate	Relative permittiv- ity of material	Relative permeabil- ity of material

The dimension of miniaturized branch line coupler is same as the dimension of branch line coupler that designed for 3 GHz. Wavelength can be calculated as

$$(3.4.1) \quad \lambda = \frac{c}{f\sqrt{\mu_r\epsilon_{eff}}}$$

where c is speed of light($c = 3 \times 10^8 m/s$), f is the operating frequency ($f = 3GHz$), μ_r is relative permeability($\mu_r = 1$) and ϵ_{eff} is effective relative permittivity ($\epsilon_{eff} = \sqrt{1.7}$.)

The design dimension of miniaturized branch line coupler is given in table 10. Labels used in the table 10 for different lengths and widths can be seen from figure 3.3.4

TABLE 10. Design parameters of miniaturized branch line coupler

l_1, l_2 (mm)	l_3, l_4 (mm)	l_f (mm)	W_1 , (mm)	W_2 , W_3 (mm)	W_f, W_4 (mm)	z_2, z_3 , z_4 , z_f (Ω)	z_1 (Ω)
19.17	4.79	17	2.5	1.52	1.52	50	35.35

The CST layout of miniaturized branch line coupler is shown in figure 3.4.2, which is designed using the dimension given in table 10

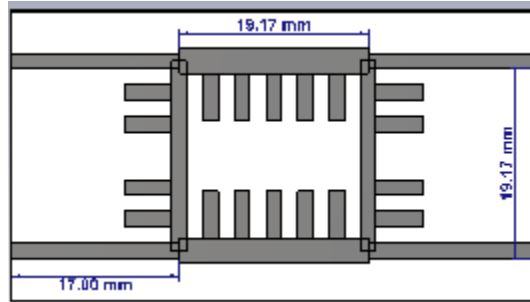


FIGURE 3.4.2. CST structure of miniaturized branch line coupler

The simulation result of the structure shown in figure 3.4.2 is given in figure 3.4.3

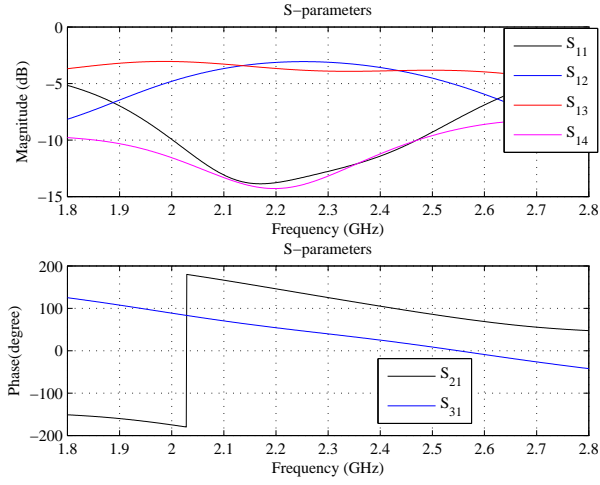


FIGURE 3.4.3. CST simulation results of miniaturized branch line coupler

Magnitude of S_{11} , S_{12} , S_{13} and S_{14} are -13.85 dB , -3.202 dB , -3.59 dB and -14.25 dB respectively at 2.163 GHz . This miniaturized branch line coupler still dividing the equal power between port 2 and port 3 and proving the angle of 92.8° between port 2 and port 3. By adding four stubs in the vertical branches and five stubs in horizontal branches of the coupler leads to the approximate size reduction of 39%

3.4.2. Validation of results. Mapping of CST simulation results with Matlab results is shown in figure 3.4.4

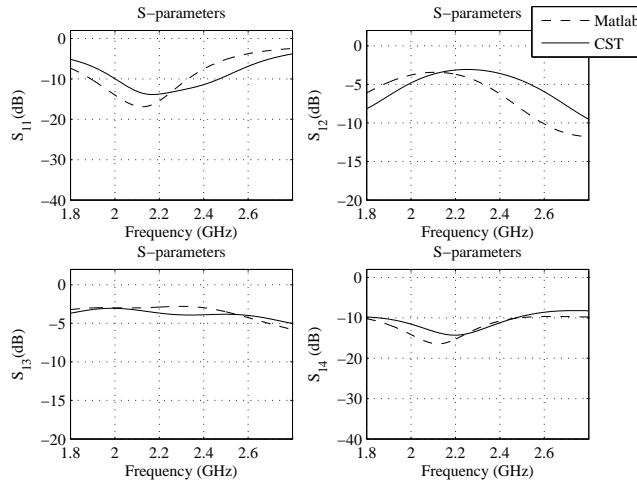


FIGURE 3.4.4. Mapping of CST and Matlab simulation results

From figure 3.4.4 this can be analyzed that scattering parameters obtained from Matlab simulations are almost matching with the scattering parameters obtained from CST simulation.

3.4.3. Branch line coupler with five stubs on vertical and horizontal branches.

Five stubs are connected in the horizontal branches and vertical branches of the coupler. Circuit diagram of branch line coupler with five horizontal stubs on each branch of the coupler is shown in figure 3.4.5

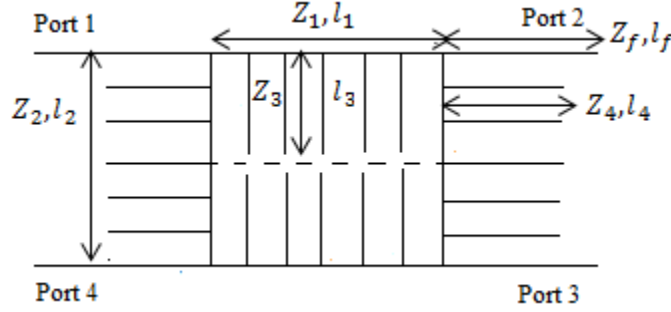


FIGURE 3.4.5. Circuit diagram of branch line coupler with five stubs on each branch

Analysis of the circuit shown in figure 3.4.5 is done in Matlab with impedance of all the added stubs taken as one (normalized by 50Ω) and length as $\frac{\lambda}{16}$. Matlab simulation results are shown in figure 3.4.1

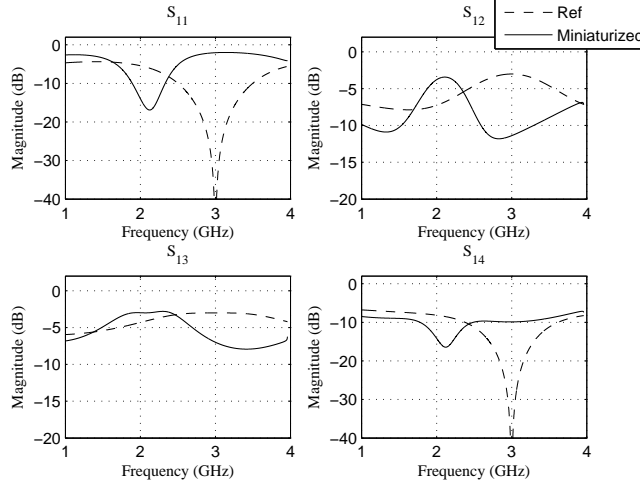


FIGURE 3.4.6. Matlab simulation result of branch line coupler with five stubs on each branch

In figure 3.4.1 comparison of modified branch line coupler (branch line coupler with five stubs in each horizontal and vertical branches) with conventional branch line coupler operating at 3 GHz is shown. The frequency of miniaturized branch line coupler is 2.121 GHz

3.4.3.1. *CST simulation result of branch line coupler with five stubs on vertical and horizontal branches.* The miniaturized branch line coupler is designed in Full wave EM simulator (CST microwave studio) [32]. The structure is placed on the material RT-Duroid 5880 which

has properties that are mentioned in table 9. The design dimensions of miniaturized branch line coupler is given in table 10. Labels used in the table 10 for different lengths and widths can be seen from figure 3.4.5. The CST layout of miniaturized branch line coupler is shown in figure 3.4.7, which is designed using the dimension given in table 10

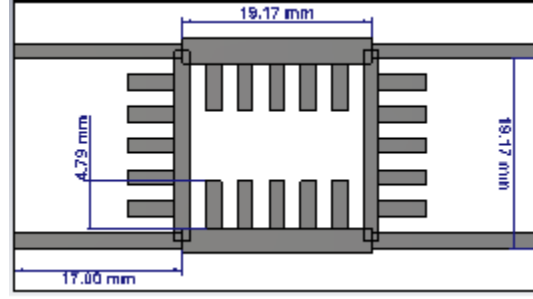


FIGURE 3.4.7. CST structure of miniaturized branch line coupler five vertical stubs on each branch

The CST simulation results of the branch line coupler with five stubs on each branch of branch line coupler is shown in figure 3.4.8

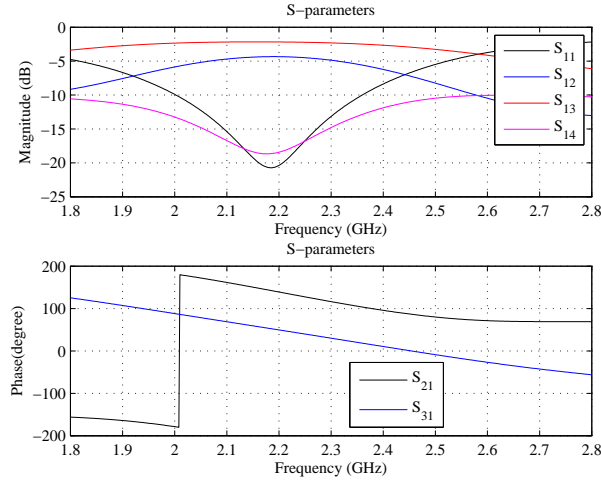


FIGURE 3.4.8. CST simulation result of miniaturized branch line coupler with five stubs on each branch

Magnitude of S_{11} , S_{12} , S_{13} and S_{14} are -20.715 dB , -4.34 dB , -2.168 dB and -18.64 dB respectively at 2.1857 GHz . This miniaturized branch line coupler still dividing the equal power between port 2 and port 3 and proving the angle of 90.04° between port 2 and port 3. By adding five stubs in the vertical and horizontal branches of the coupler leads to the approximate size reduction of 37 %.

3.4.4. Validation of results. Mapping of CST simulation results with Matlab results is shown in figure 3.4.9

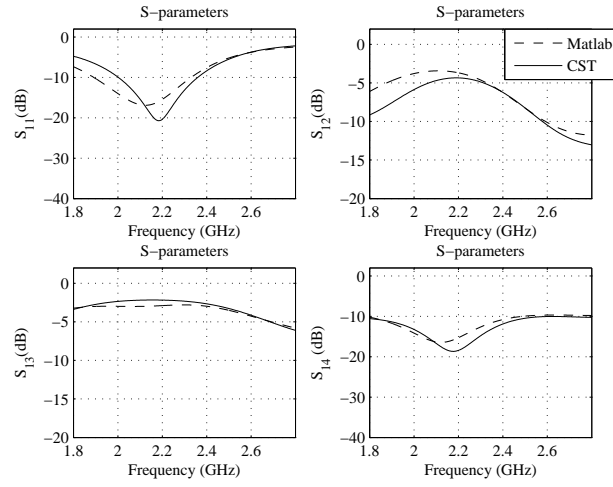


FIGURE 3.4.9. Mapping of CST and Matlab simulation results of miniaturized BLC

From figure 3.4.9 this can be analyzed that scattering parameters obtained from Matlab simulations are almost matching with the scattering parameters obtained from CST simulation.

CHAPTER 4

REALIZATION OF WIDE BAND BRANCH LINE COUPLER USING FILTERS COEFFICIENTS

One of the motive of this research work is to make wide band branch line coupler and for this purpose time delay has to be minimized so that phase variation is almost constant. The relation between time delay and phase is given as

$$(4.0.1) \quad \phi = 2\pi f t_d$$

where ϕ is the phase, f is the frequency, t_d is the time delay.

From equation 1.2 it can be seen that t_d is inversely proportional to v_p , so to reduce time delay v_p should be increased.

$$(4.0.2) \quad t_d = \frac{l}{v_p}$$

where t_d is the delay, l is the length, v_p is the phase velocity.

The phase velocity can be expressed as

$$(4.0.3) \quad v_p = \frac{1}{\sqrt{LC}}$$

where L is inductance and C is the capacitance.

To minimize t_d , phase velocity v_p can be increased. To increase v_p the capacitance and inductance can be reduced. If capacitance reduces width of the transmission line section reduces. If width reduces impedance increases.

To make wide band branch line coupler firstly the horizontal branches of branch line coupler are replaced with filter coefficients. Impedance of the coupler is increased further such that maximum impedance have a value which is practical to fabricate so in this analysis maximum impedance value is restricted to 150Ω . Comparison of replacing the branch line coupler with filter coefficients of Butterworth, Equiripple and Binomial filters are done. This analysis is carried out with third and fifth order coefficients of aforementioned filters. Replacing the branch line coupler's horizontal line with third order filter coefficients and fifth order filter coefficients divides the coupler's horizontal branch in three and five equal lengths respectively.

4.1. Branch line coupler with third order filters

The prototype value for Butterworth (Maximally flat low pass filter) , Equiripple low pass filters are taken from table 8.3 and 8.4 of [3]. Coefficient of third order binomial filter is same as Butterworth third order filter, so for third order filter comparison between the Butterworth, Equiripple and branch line coupler is shown in figure 4.1.1. Basic idea is to make branch line coupler wide band and taking the output from the port 3 and port 4 (isolated port).

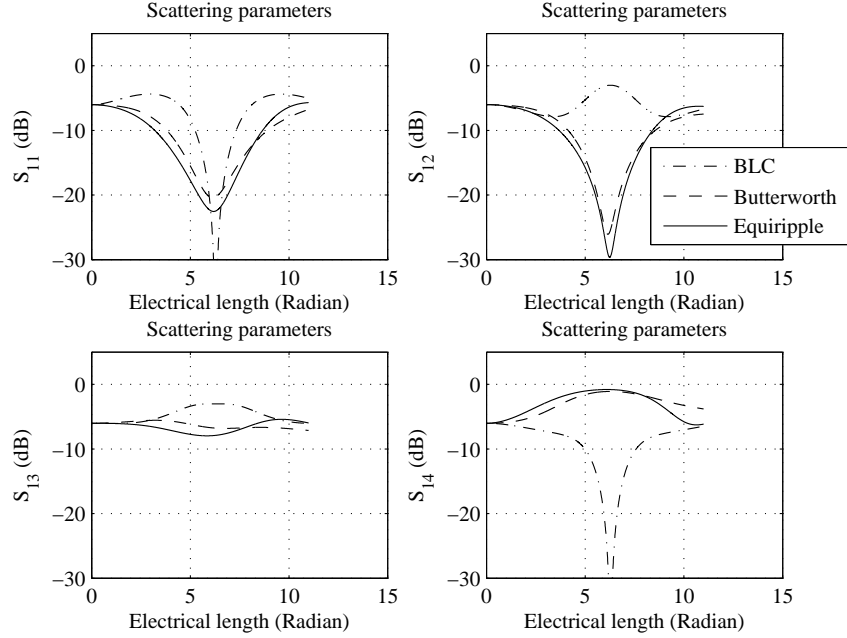


FIGURE 4.1.1. Matlab simulation results of BLC with third order filter

Comparison of fractional bandwidth between the Butterworth, Equiripple and branch line coupler is shown in table 1.

TABLE 1. Comparison of BLC with 3rd order filters

Filter	S_{13}	S_{14}	Bandwidth	Fractional Bandwidth (%)	Electrical length (Radian)
Butterworth	0.5211	0.8817	5.1080	83.21	6.13
Equiripple (0.5dB)	0.5365	0.9123	5.4610	88.33	6.18
BLC	0.707	0	2.287	36.41	6.28

It is clear from the table 1 that fractional bandwidth of Equiripple filter is more than conventional branch line coupler and Butterworth third order filter. Power is divided between the port 4 and port 3. More power is directed toward port 4.

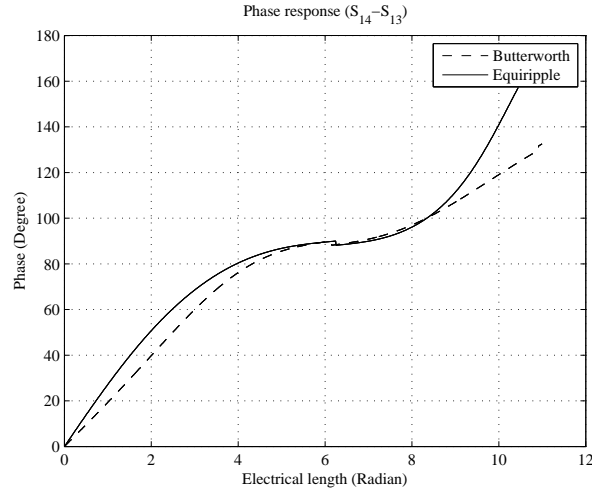


FIGURE 4.1.2. Phase response of BLC with third order Butterworth and Equiripple filters

From figure 4.1.2 it can be seen that in angle between port 4 and port 3 is 90° .

4.2. Branch line coupler with fifth order filters

Horizontal branches of branch line coupler are replaced by fifth order filter coefficients of Butterworth, Equiripple and Binomial filter. Then comparison of conventional branch line coupler with all the cases (replacing the horizontal branch with three filter coefficient) is done in figure 4.2.1

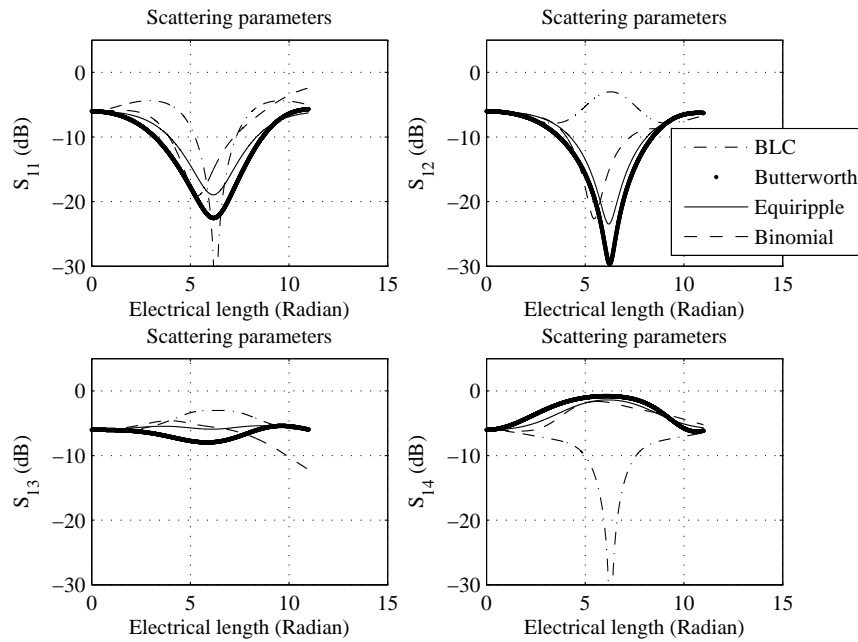


FIGURE 4.2.1. Matlab simulation results of BLC with fifth order filters

Table 2 shows the gains at port 3 and port 4, when horizontal branches of branch line coupler are replaced with Butterworth, Equiripple and Binomial fifth order filters and comparison of fractional bandwidth between the Butterworth, Equiripple and branch line coupler is also shown.

TABLE 2. Comparison of BLC with 5th order filters

Filter	S_{13}	S_{14}	Bandwidth	Fractional Bandwidth (%)	Electrical length (Radian)
Butterworth	0.5338	0.8817	4.869	82.65	5.8912
Binomial	0.5887	0.8296	3.2790	60.93	5.3820
Equiripple (0.5dB)	0.5380	0.8524	4.335	70.29	6.1674
BLC	0.707	0	2.287	36.41	6.28

From table 2 it is clear that factional bandwidth is more when horizontal branches of branch line coupler are replaced with filter coefficients of Butterworth fifth order filter.

Figure 4.2.2 shows the phase response of branch line coupler when replaced with the filter coefficients of Butterworth, Equiripple and Binomial fifth order filters.

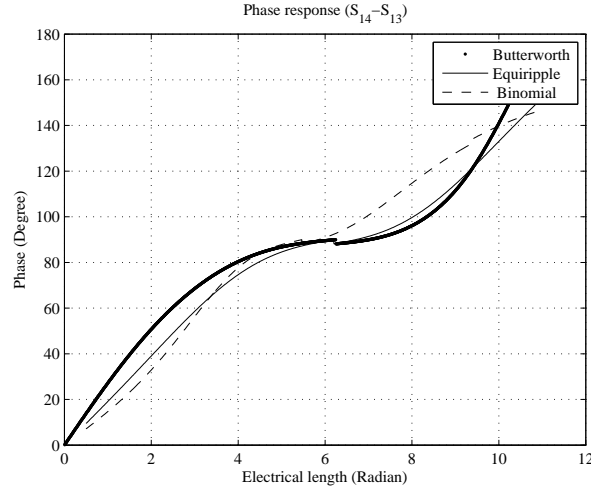


FIGURE 4.2.2. Phase response of BLC replaced with Butterworth, Equiripple and Binomial fifth order filters

From figure 4.2.2 it can be seen that in angle between port 4 and port 3 is 90° .

Replacing the branch line coupler's horizontal line with third order filter coefficients and fifth order filter coefficients divides the power between port 4 and port 3. If vertical branches of the coupler is replaced with filter coefficients then power will be divided between port 2 and port 3.

Unequal power division which is useful in beam forming networks is generally achieved by changing the impedance of the complete horizontal line. But changing the impedance of a

small part of branch line coupler can give unequal power division at the output port. A simple design for unequal power division is discussed in the next chapter.

CHAPTER 5

IMPEDANCE VARIATION OF BRANCH LINE COUPLER

To study the effect of impedance variation of branch line coupler firstly the horizontal branch of a branch line coupler is divided into three equal parts which can be visualized from figure 5.0.1.

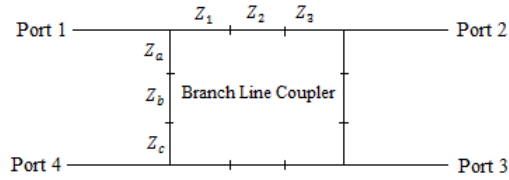


FIGURE 5.0.1. Circuit of branch line coupler for impedance variation

Then original impedance of the whole horizontal line of branch line coupler is scaled by different Impedance values. The range of these impedance values is chosen in such a way that the S_{11} and S_{41} of the branch line coupler remain below -10 dB . Then the effect of this impedance variation is observed on the S-parameters of branch line coupler. As S_{11} and S_{41} are below -10 dB so the reflection coefficients of branch line coupler are well taken care of, so only the variation of S_{21} and S_{31} are shown in the figure 5.0.2

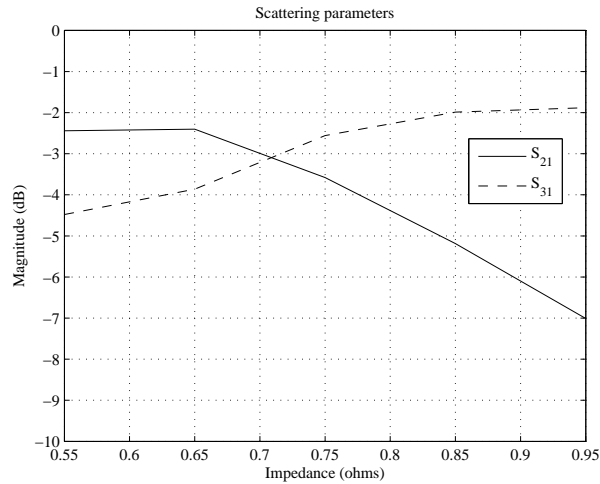


FIGURE 5.0.2. Variation of S-parameters of BLC with varying impedance of complete horizontal line

From figure 5.0.2 it can be seen that as impedance value is increasing S_{21} is decreasing and S_{31} is increasing. By changing the impedance of branch line coupler power distribution between port 2 and port 3 can be controlled. The resonance frequency is constant for all impedance values.

5.1. Variation in impedance of middle line of branch line coupler

Unequal power distribution can also be achieved by varying the impedance of middle line of the branch line coupler. Instead of changing the impedance of the complete horizontal line, variation in the impedance middle line (that is Z_2 in figure 5.0.1) of the horizontal branch of the coupler is done. The range of impedance is chosen such that the S_{11} and S_{14} of branch line coupler are less than -8 dB. Effect of these impedance variations on S_{12} and S_{13} are observed in figure 5.1.1.

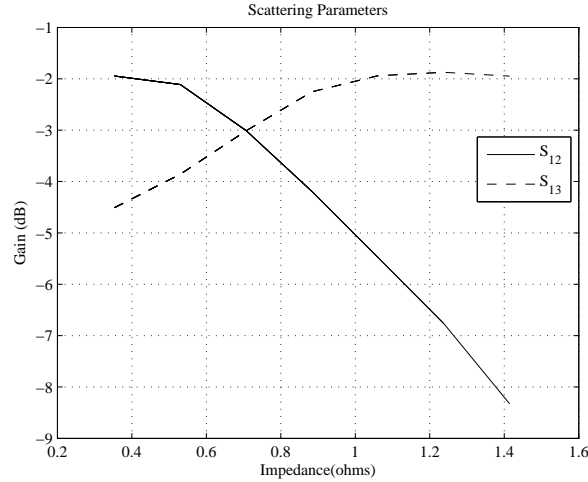


FIGURE 5.1.1. Variation of S-parameters of BLC with impedance variation

It can be depicted from figure 5.1.1 that S_{12} starts decreasing and S_{13} starts increasing after the impedance value of Z_2 in figure 5.0.1 increases from the impedance of the simple branch line coupler (i.e 35.35Ω). The maximum value of impedance that satisfies the condition of S_{11} and S_{14} being less than -8 dB is two (normalized with 50Ω).

Circuit diagram of modified branch line coupler is given in figure 5.1.2. By changing the impedance Z_2 of the line l_2 , unequal power division can be achieved. If modified branch line coupler is used in antenna array then amplitude tapering is possible but with conventional branch line coupler amplitude tapering is not possible as it provide equal gain on both the output ports .

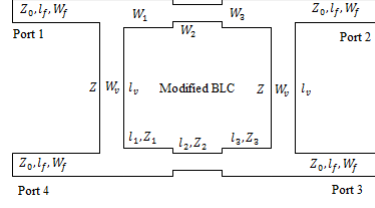


FIGURE 5.1.2. Circuit diagram of modified branch line coupler

Impedance Z_2 (in figure 5.1.2) of the middle line is varied and effect of the impedance change on the output of the branch line coupler is analyzed. In figure 5.1.2

$$(5.1.1) \quad l_1 = l_2 = l_3 = l_h$$

$$(5.1.2) \quad Z_1 = Z_3 = \frac{Z_0}{\sqrt{2}}$$

$$(5.1.3) \quad Z_2 = \frac{2Z_0}{\sqrt{2}}$$

Impedance Z_2 of the modified branch line coupler is double the impedance of horizontal side of conventional branch line coupler.

Figure 5.1.3 shows the modified branch line coupler layout designed in Full wave EM simulator (CST microwave studio) [32]. The structure is placed on the material RT-Duroid 5880 which has properties that are mentioned in table 9.

The modified branch line coupler is designed for 3 GHz. Wavelength can be calculated as

$$(5.1.4) \quad \lambda = \frac{c}{f\sqrt{\mu_r\epsilon_{eff}}}$$

where c is speed of light($c = 3 \times 10^8$)m/s, f is the operating frequency ($f = 3GHz$), μ_r is relative permeability($\mu_r = 1$) and ϵ_{eff} is effective relative permittivity ($\epsilon_{eff} = \sqrt{1.7}$.)

The design dimension of modified branch line coupler is as follows

TABLE 1. Design parameters of modified branch line coupler

l_h (mm)	l_v (mm)	l_f (mm)	W_1, W_3 (mm)	W_2 (mm)	W_f, W_v (mm)	z_0, z (Ω)	z_1, z_3 (Ω)	z_2 (Ω)
6.39	19.17	17	2.5	0.85	1.52	50	35.35	70.7

Port locations of modified branch line coupler in figure 5.1.3 is same as conventional branch line coupler.

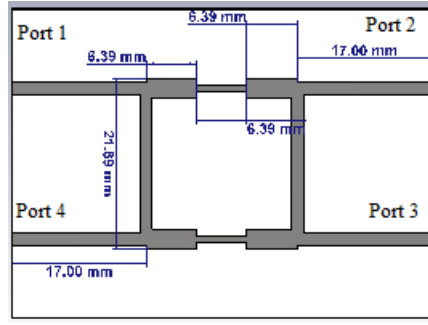


FIGURE 5.1.3. CST layout of modified BLC

CST simulation results of modified branch line coupler and conventional branch line coupler is given in figure 5.1.4.

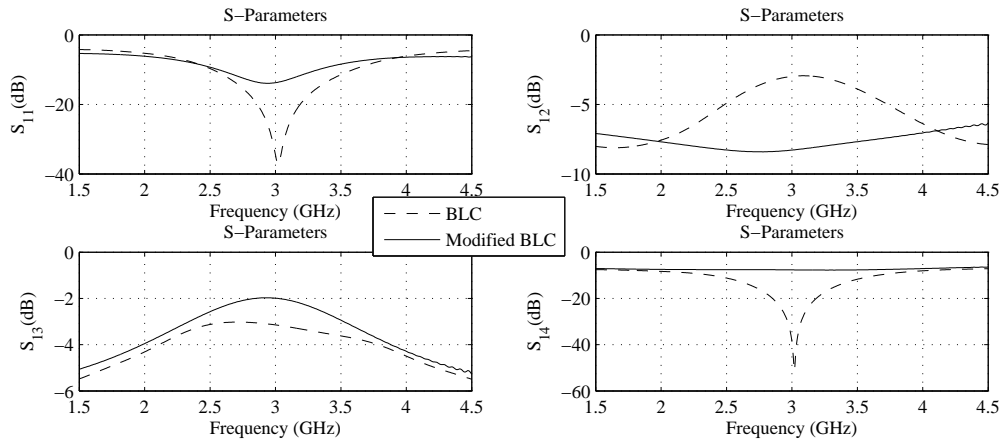


FIGURE 5.1.4. Simulation results of conventional and modified branch line coupler

From figure 5.1.4 it can be observed that S_{12} and S_{13} of conventional branch line coupler is -2.99 dB and -3.22 dB where as S_{12} and S_{13} of modified branch line coupler is -8.32 dB and -1.97 dB respectively. There is approximately 6 dB difference between S_{12} and S_{13} of modified branch line coupler.

Figure 5.1.5 shows the phase response of conventional and modified branch line coupler.

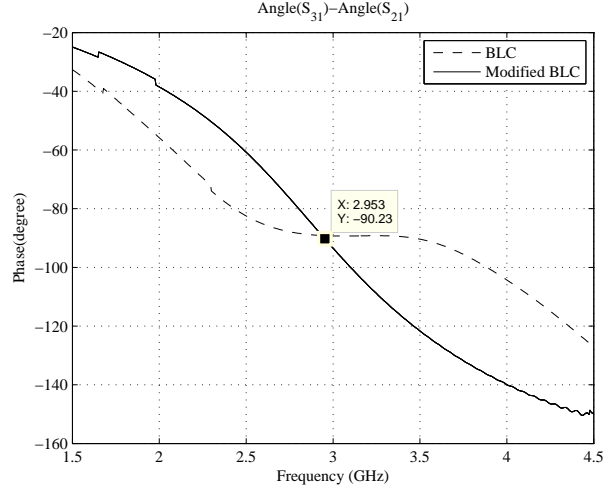


FIGURE 5.1.5. Phase responses of conventional and modified branch line coupler

Angles of S_{12} and S_{13} of conventional branch line coupler are 102.5^0 and 12.73^0 . The difference between the two is 89.626^0 . Angles of S_{12} and S_{13} of modified branch line coupler are 103.369^0 and 13.05^0 respectively. Difference between the two is 90.3^0 . From this analysis it can be said that there is not much difference between the phase provided by conventional and modified branch line coupler at their two output ports.

5.1.1. Application of modified branch line coupler. Modified branch line coupler can be utilized in antenna arrays. To utilize the modified branch line coupler in antenna arrays firstly two modified branch line coupler are needed. One would be the mirror image of the other. It can be more clearly visualized from figure 5.1.6. If adjacent ports of two modified branch line coupler are excited simultaneously then difference pattern can be obtained. If two distant ports are excited simultaneously then sum pattern can be obtained. Sum and difference patterns are used in target detection

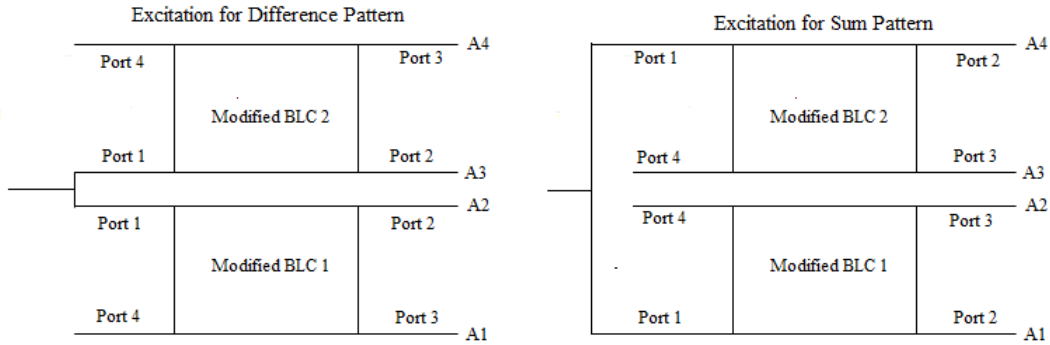


FIGURE 5.1.6. Excitation for difference and sum patterns using modified BLC in antenna arrays

Figure 5.1.7 shows the comparison between sum and difference patterns of three cases. First case is when simple antenna array is used instead of couplers (in figure 5.1.6), second is when branch line coupler is used in the configuration shown in figure 5.1.6 and the last one is when modified branch line coupler is used in the configuration shown in figure 5.1.6

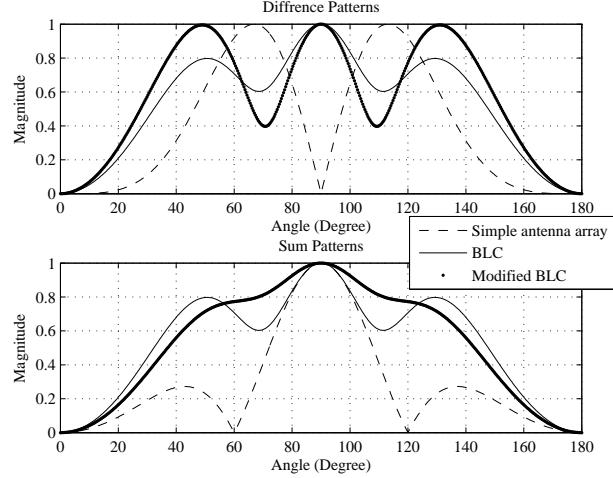


FIGURE 5.1.7. Sum and difference pattern of simple antenna array, conventional branch line coupler and modified branch line coupler

From figure 5.1.7 it can be seen that magnitude of sum and difference patterns of conventional branch line coupler are exactly same. The difference between the sum and difference patterns is zero which is shown in figure 5.1.8. For target detection there has to be two different plots of sum and difference patterns. Hence target detection is not possible in this case.

TABLE 2. Phase and gain of sum and difference patterns of simple BLC

Sum Pattern	A1	A2	A3	A4
Magnitude	0.7071	0.7071	0.7071	0.7071
Phase	-90^0	-180	-180	-90^0
Difference Pattern	A1	A2	A3	A4
Magnitude	0.7071	0.7071	0.7071	0.7071
Phase	-180^0	-90^0	-90^0	-180^0

From table 2 it can be observed that simple branch line coupler does not provide amplitude tapering.

Advantage of using modified branch line coupler over simple branch line coupler is that here two different plots are obtained corresponding to sum and difference patterns so target detection is possible in this case.

TABLE 3. Phase and gain of sum and difference patterns of modified BLC

Sum Pattern	A1	A2	A3	A4
Magnitude	0.3867	0.7937	0.7937	0.3867
Phase	-92.08^0	-171.45^0	-171.45^0	-92.08^0
Difference Pattern	A1	A2	A3	A4
Magnitude	0.7937	0.3867	0.3867	0.7937
Phase	-171.45^0	-92.08^0	-92.08^0	-171.45^0

From the table 3 it can be seen that the amplitude tapering is also possible from modified branch line coupler.

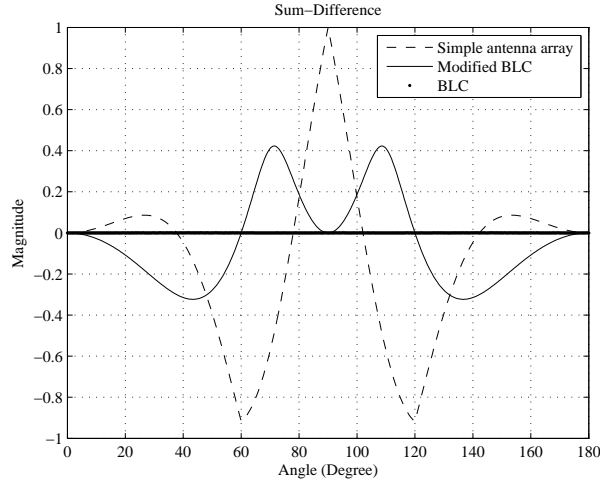


FIGURE 5.1.8. Difference between sum and difference patterns

Modified branch line coupler difference pattern has three beams as shown in figure 5.1.7 because of which we can divide the slope in three regions for target detection as shown in table 4.

TABLE 4. Regions for target detection with modified branch line coupler in antenna array

	Region 1	Region 2	Region 3
X(Angle)	(5^0) to (43.2^0)	(43.2^0) to (71.28^0)	(71.28^0) to (90^0)
Y(Magnitude)	(-0.008083) to (-0.3232)	(-0.3232) to (0.4227)	(0.4227) to (0)

Although there are already different antenna array which provide sum and difference patterns for target detection. But from the figure 5.1.8 it is visible that for target detection this graph can be divided into two regions. In other words there are only two slopes in which target can be detected as shown in table 5. In other words there are only two slopes in which target can be detected.

TABLE 5. Regions for target detection in simple antenna array

	Region 1	Region 2
X(Angle)	(26.64 ⁰) to (60.12 ⁰)	(60.12 ⁰) to (90 ⁰)
Y(Magnitude)	(0.08365) to (−0.9171)	(−0.9171) to (1)

From the analysis it can be observed that by changing the impedance of the the middle line there is little or no change in the phase property of the coupler. It has the effect on the gain. In modified branch line coupler only S_{13} is high and S_{11} , S_{12} , S_{14} are low. Which mean all the output is coming from port 3. Hence with the small variation in the impedance of branch line coupler unequal power division can be achieved. It can be utilized in radar system for detecting the objects.

- Advantage of modified branch line coupler over conventional branch line coupler is that it provide amplitude tapering which simple branch line coupler does not provide.
- Simple branch line coupler can not be used for target detection as the sum and difference patterns of simple branch line coupler are exactly same.
- Advantage of modified branch line coupler over simple antenna array is that in modified branch line coupler difference pattern has three beams because of which we can divide the slope in three regions for target detection.

Hence small impedance variation in conventional branch line coupler can lead to various advantages.

CHAPTER 6

CONCLUSION

In this research work, the analysis of branch line coupler is done considering the three aspects of branch line coupler that are, to miniaturization branch line coupler, to make wide band branch line coupler and utilizing the branch line coupler for unequal power division.

For miniaturization, analysis of branch line coupler is done by changing three parameters that are number of stub, length of stub and impedance of stub. Simulation is done by varying all the parameters one by one and their effects are evaluated. It can be concluded that when the stubs are added in the branch line coupler, the resonance frequency of the coupler is decreasing, thus by adding four stubs in vertical and five stubs in horizontal branches of branch line coupler, 39% of size reduction is achieved. This miniaturized structure can be used where circuit size is big issue.

The other modification in the branch line coupler is done by replacing the horizontal branches of the coupler with Butterworth filter coefficients. By doing this, the fractional bandwidth of modified branch line coupler is more than 80%.

Unequal power division can be achieved by small variation in the impedance of branch line coupler. This system can be utilized in radar system for detecting the objects. Advantage of modified branch line coupler over conventional branch line coupler is that it provide amplitude tapering which simple branch line coupler does not provide.

Bibliography

- [1] R. E. Collin, *Foundations for microwave engineering*. John Wiley & Sons, 2007.
- [2] V. K. Varadan, K. J. Vinoy, and K. A. Jose, *RF MEMS and their applications*. John Wiley & Sons, 2003.
- [3] D. M. Pozar, *Microwave engineering*. John Wiley & Sons, 2009.
- [4] L. Sun, Y.-Z. Yin, X. Lei, and V. Wong, “A novel miniaturized branch-line coupler with equivalent transmission lines,” *Progress In Electromagnetics Research*, vol. 38, pp. 35–44, 2013.
- [5] B. Li, X. Wu, and W. Wu, “A miniaturized branch-line coupler with wideband harmonics suppression,” *Progress In Electromagnetics Research*, vol. 17, pp. 181–189, 2010.
- [6] H.-y. Zeng, G.-m. Wang, Z.-w. Yu, X.-k. Zhang, and T.-p. Li, “Miniaturization of branch-line coupler using composite right/left-handed transmission lines with novel meander-shaped-slots cssrr,” *Radioengineering*, vol. 21, no. 2, pp. 606–610, 2012.
- [7] C.-W. Tang, M.-G. Chen, and C.-H. Tsai, “Miniaturization of microstrip branch-line coupler with dual transmission lines,” *IEEE Microwave and Wireless Components Letters*, vol. 18, no. 3, pp. 185–187, 2008.
- [8] H. Kim, B. Lee, and M.-J. Park, “Dual-band branch-line coupler with port extensions,” *IEEE Transactions on Microwave Theory and Techniques*, vol. 58, no. 3, pp. 651–655, 2010.
- [9] K. W. Eccleston and S. H. Ong, “Compact planar microstripline branch-line and rat-race couplers,” *IEEE Transactions on microwave theory and techniques*, vol. 51, no. 10, pp. 2119–2125, 2003.
- [10] J. Zhu, Y. Zhou, and J. Liu, “Miniaturization of broadband 3-db branch-line coupler,” *Progress In Electromagnetics Research*, vol. 24, pp. 169–176, 2011.
- [11] S. Velan, S. Kingsly, M. Kanagasabai, M. G. N. Alsath, Y. P. Selvam, and S. Subbaraj, “Quad-band rat-race coupler with suppression of spurious pass-bands,” *IEEE Microwave and Wireless Components Letters*, vol. 26, no. 7, pp. 490–492, 2016.
- [12] J.-S. Kim and K.-B. Kong, “Compact branch-line coupler for harmonic suppression,” *Progress In Electromagnetics Research*, vol. 16, pp. 233–239, 2010.
- [13] W. A. Arriola, J. Y. Lee, and I. S. Kim, “Wideband 3 db branch line coupler based on lambda/4 open circuited coupled lines,” *IEEE microwave and wireless components letters*, vol. 21, no. 9, pp. 486–488, 2011.
- [14] S. Lee and Y. Lee, “Wideband branch-line couplers with single-section quarter-wave transformers for arbitrary coupling levels,” *IEEE Microwave and Wireless Components Letters*, vol. 22, no. 1, pp. 19–21, 2012.
- [15] M. A. Maktoomi, M. S. Hashmi, and F. M. Ghannouchi, “Systematic design technique for dual-band branch-line coupler using t-and pi-networks and their application in novel wideband-ratio crossover,” *IEEE Transactions on Components, Packaging and Manufacturing Technology*, vol. 6, no. 5, pp. 784–795, 2016.
- [16] H.-J. Yoon and B.-W. Min, “Two section wideband 90° hybrid coupler using parallel-coupled three-line,” *IEEE microwave and wireless components letters*, vol. 27, no. 6, pp. 548–550, 2017.
- [17] Q. Wu, Y. Yang, Y. Wang, X. Shi, and M. Yu, “Characteristic impedance control for branch-line coupler design,” *IEEE Microwave and Wireless Components Letters*, 2018.

- [18] R. Gomez-Garcia, J. I. Alonso, and D. Amor-Martin, "Using the branch-line directional coupler in the design of microwave bandpass filters," *IEEE transactions on microwave theory and techniques*, vol. 53, no. 10, pp. 3221–3229, 2005.
- [19] J.-Q. Gong, C.-H. Liang, and B. Wu, "Compact dual-band 90° couplers with customizable power division ratios utilizing scrh transmission lines," *Progress In Electromagnetics Research*, vol. 36, pp. 29–40, 2013.
- [20] G. Lian, Z. Wang, Z. He, Z. Zhong, L. Sun, and M. Yu, "A new miniaturized microstrip branch-line coupler with good harmonic suppression," *Progress In Electromagnetics Research*, vol. 67, pp. 61–66, 2017.
- [21] I. Prudyus and V. Oborzhytskyy, "Design of dual-band two-branch-line couplers with arbitrary coupling coefficients in bands," *Radioengineering*, vol. 23, no. 4, pp. 1099–1108, 2014.
- [22] I. Sakagami, M. Fujii, and T. Wuren, "Impedance-transforming lumped element two-branch 90° couplers in case of type c," in *Proc. 10th WSEAS Int. Conf. Circuits, Vouliagmeni, Athens, Greece, July*, pp. 10–12, Citeseer, 2006.
- [23] D. Baatarkhuu, B. Myagmarsuren, and R. Baigalmaa, "A new design method for a dual band branch line hybrid coupler," *Mongolian Journal of Agricultural Sciences*, vol. 15, no. 2, pp. 152–158, 2015.
- [24] V. K. Kothapudi, V. Kumar, D. A. Preetham, and M. S. Rohit, "Design and fabrication of 430mhz unequal amplitude hybrid coupler for t-radar beam forming unit," *Indian Journal of Science and Technology*, vol. 9, no. 36, 2016.
- [25] Y. Wu, Y. Liu, Q. Xue, S. Li, and C. Yu, "Analytical design method of multiway dual-band planar power dividers with arbitrary power division," *IEEE Transactions on Microwave Theory and Techniques*, vol. 58, no. 12, pp. 3832–3841, 2010.
- [26] M.-J. Park and B. Lee, "Design of ring couplers for arbitrary power division with 50 ohms lines," *IEEE Microwave and Wireless Components Letters*, vol. 21, no. 4, pp. 185–187, 2011.
- [27] H. Oraizi and A.-R. Sharifi, "Optimum design of asymmetrical multisection two-way power dividers with arbitrary power division and impedance matching," *IEEE Transactions on Microwave Theory and Techniques*, vol. 59, no. 6, pp. 1478–1490, 2011.
- [28] W. Choe and J. Jeong, "*n*-way unequal wilkinson power divider with physical output port separation," *IEEE Microwave and Wireless Components Letters*, vol. 26, no. 4, pp. 243–245, 2016.
- [29] M. A. Maktoomi, M. S. Hashmi, and F. M. Ghannouchi, "A dual-band port-extended branch-line coupler and mitigation of the band-ratio and power division limitations," *IEEE Transactions on Components, Packaging and Manufacturing Technology*, vol. 7, no. 8, pp. 1313–1323, 2017.
- [30] J. Lee, J. Lee, and M.-J. Park, "Branch-line couplers with arbitrary coupling value through the electrical length variation with fixed line impedances," *IEEE Microwave and Wireless Components Letters*, vol. 27, no. 11, pp. 968–970, 2017.
- [31] R. Rao, *Microwave engineering*. PHI Learning Pvt. Ltd., 2015.
- [32] CSTMicrowaveStudio, *Studentversion 2017*. Darmstadt, Germany: 3D EM Application Team Infineon Technologies AG, 2017.
- [33] MATLAB, *version 7.10.0 (R2013a)*. Natick, Massachusetts: The MathWorks Inc., 2013.